

Community detection in multi-layer bipartite networks

Huan Qing^{a,*}

^a*School of Economics and Finance, Lab of Financial Risk Intelligent Early Warning and Modern Governance, Chongqing University of Technology, Chongqing, 400054, China*

Abstract

The problem of community detection in multi-layer undirected networks has received considerable attention in recent years. However, practical scenarios often involve multi-layer bipartite networks, where each layer consists of two distinct types of nodes. Existing community detection algorithms tailored for multi-layer undirected networks are not directly applicable to multi-layer bipartite networks. To address this challenge, this paper introduces a novel multi-layer degree-corrected stochastic co-block model specifically designed to capture the underlying community structure within multi-layer bipartite networks. Within this framework, we propose an efficient debiased spectral co-clustering algorithm for detecting nodes' communities. We establish the consistent estimation property of our proposed algorithm and demonstrate that an increased number of layers in bipartite networks improves the accuracy of community detection. Through extensive numerical experiments, we showcase the superior performance of our algorithm compared to existing methods. Additionally, we validate our algorithm by applying it to real-world multi-layer network datasets, yielding meaningful and insightful results.

Keywords: Multi-layer bipartite networks, community detection, debiased spectral co-clustering, multi-layer degree-corrected stochastic co-block model, asymptotic analysis

1. Introduction

In network analysis, multi-layer networks have emerged as ubiquitous structures in the real world, encompassing diverse systems from social networks to biological interactions (De Domenico et al., 2013; Kivelä et al., 2014; Boccaletti et al., 2014; De Domenico et al., 2015a, 2016; Pilosof et al., 2017). These networks, characterized by multiple layers, offer a rich framework for understanding the complex relationships and interactions within and across various systems. For instance, users connect with each other on different platforms such as email, messaging, Facebook, Twitter, Instagram, and WeChat (Papalexakis et al., 2013), where each platform denotes a layer. Similarly, in biological systems, different layers record genes' co-expression relationships of the animal at different developmental stages (Narayanan et al., 2010; Bakken et al., 2016; Zhang & Cao, 2017).

In recent years, the problem of community detection in multi-layer networks has garnered significant attention. Community detection aims to identify groups of nodes that are tightly interconnected within each group but relatively sparsely connected to nodes in other groups (Girvan & Newman, 2002; Newman & Girvan, 2004; Fortunato, 2010; Papadopoulos et al., 2012; Fortunato & Hric, 2016; Javed et al., 2018). The significance of community detection in multi-layer networks lies in its ability to reveal hidden structures and patterns that may not be evident from a single-layer analysis (Lei & Lin, 2023). By accounting for the richness of interactions in multiple layers, researchers can gain a more comprehensive understanding of the system's overall behavior (Kim & Lee, 2015; Huang et al., 2021). This, in turn, has led to a surge in research efforts aimed at developing effective and efficient algorithms for community detection in multi-layer networks.

An extensively studied version of this problem assumes that each layer of the multi-layer network is derived from the classical stochastic block model (SBM) (Holland et al., 1983). This model assumes that the probability of an edge

*Corresponding author.

Email address: qinghuan@u.nus.edu & qinghuan07131995@163.com & qinghuan@cqut.edu.cn (Huan Qing)

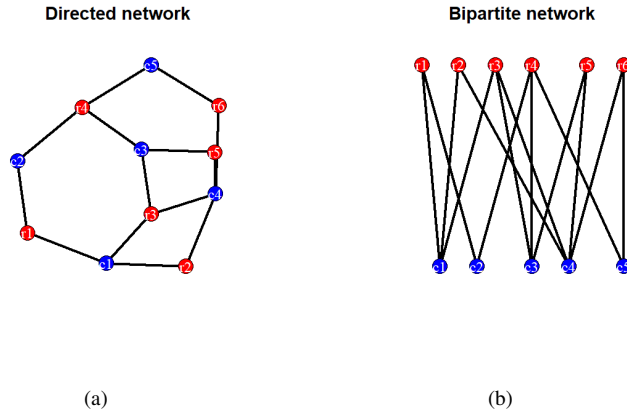


Figure 1: A toy example of transforming a directed network in panel (a) to a bipartite network in panel (b). In both panels, red dots and blue dots represent row nodes and column nodes, respectively.

forming between two nodes is solely determined by their respective communities, with nodes belonging to the same community exhibiting similar connectivity patterns. (Han et al., 2015) conducted an asymptotic analysis of a spectral clustering algorithm and a maximum likelihood method by increasing the number of layers while fixing the number of nodes within the context of the multi-layer SBM. (Paul & Chen, 2020) focused on the consistent community detection of spectral and matrix factorization methods under the multi-layer SBM. (Lei et al., 2020) proposed a least-squares estimation technique and provided its theoretical guarantees of consistency within the multi-layer SBM framework. (Jing et al., 2021) introduced a mixture multi-layer SBM and developed a tensor-based approach for identifying the community memberships of both nodes and layers. (Fan et al., 2022) proposed an alternating minimization algorithm that outperforms the tensor-based method in (Jing et al., 2021) both theoretically and numerically under the mixture multi-layer SBM introduced in (Jing et al., 2021). (Chen & Mo, 2022) introduced a multi-layer weighted SBM to model multi-layer weighted networks and fitted this model by a variational expectation-maximization algorithm. (Lei & Lin, 2023) developed an efficient debiased spectral clustering method that significantly outperforms methods considered in (Paul & Chen, 2020) and established its theoretical guarantees within the multi-layer SBM framework.

While the multi-layer SBM is powerful in modeling multi-layer networks with latent community structures, it assumes that the interactions between nodes are symmetric or undirected, limiting its ability to capture community patterns in multi-layer directed networks. To take into the asymmetry in multi-layer directed networks, (Su et al., 2023) proposed a multi-layer stochastic co-block model (multi-layer ScBM) and developed an efficient, theoretically consistent debiased spectral co-clustering approach to detect communities. This model assumes that each layer of the multi-layer directed network is generated from the stochastic co-block model (ScBM) introduced in (Rohe et al., 2016). On the one hand, since directed networks naturally generalize to bipartite networks (also known as two-mode networks), where a bipartite network contains two types of nodes, and edges exist solely between nodes of different types (Latapy et al., 2008; Rohe et al., 2016; Vasques Filho & O’Neale, 2018), theoretical results in (Su et al., 2023) are only suited for multi-layer directed networks and inapplicable for multi-layer bipartite networks. Figure 1 provides an illustrative example of transforming a directed network into a bipartite network. Figure 2 illustrates an example of a multi-layer bipartite network, consisting of three layers. On the other hand, the multi-layer ScBM assumes that nodes within the same communities share similar connectivity patterns and does not consider the degree heterogeneity of nodes while nodes have various degrees in real-world networks (Karrer & Newman, 2011). To address this, the degree-corrected stochastic block model (DCSBM) proposed by (Karrer & Newman, 2011) introduced degree heterogeneity parameters, extending SBM to networks with heterogeneous degrees. Similarly, the degree-corrected stochastic co-block model (DC-ScBM) in (Rohe et al., 2016) extended DCSBM to bipartite networks. Given these limitations of the multi-layer ScBM considered in (Su et al., 2023), this paper focuses on the problem of community detection in multi-layer bipartite networks by assuming that each layer of a multi-layer bipartite network is generated from DC-ScBM and developing an efficient method to detect nodes’ communities. Our main contributions are as follows:

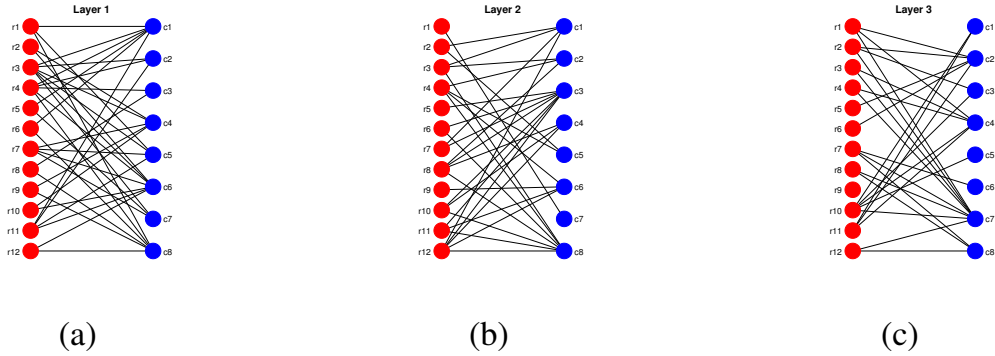


Figure 2: A multi-layer bipartite network with 12 row nodes, 8 column nodes, and 3 layers.

- We introduce the multi-layer degree-corrected stochastic co-block model (multi-layer DC-ScBM), a highly flexible network model designed to capture the latent community structures within multi-layer bipartite networks. This model encompasses numerous previous models, including the multi-layer ScBM, multi-layer SBM, DC-ScBM, ScBM, DCSBM, and SBM, as specific cases.
- To detect nodes' communities within the framework of the multi-layer DC-ScBM for multi-layer bipartite networks, we propose an efficient debiased spectral co-clustering method. Specifically, we apply the K-means algorithm to the row-normalized versions of a select few top eigenvectors of two debiased matrices, enabling us to accurately identify the community memberships of nodes. To the best of our knowledge, our study is the first to investigate the community detection problem within the context of the multi-layer DC-ScBM for multi-layer bipartite networks.
- We establish the consistency of our method by providing theoretical upper bounds for its clustering errors as the number of nodes and/or layers increases under the multi-layer DC-ScBM. Our theoretical findings underscore the benefits of incorporating multiple layers in community detection tasks.
- Through simulated data, we demonstrate that our method significantly surpasses state-of-the-art community detection methods for multi-layer bipartite networks. Furthermore, real-world data examples illustrate the practical utility of our proposed method, yielding meaningful and insightful results.

The rest of this paper is structured as follows. Section 2 describes the model. Section 3 presents the proposed method. Section 4 establishes its consistency. Section 5 offers simulations to demonstrate its effectiveness. Section 6 includes applications using real-world data. Section 7 concludes. Technical proofs are given in Appendix A.

Notation. For brevity, we denote the set $\{1, 2, \dots, m\}$ as $[m]$ and the $m \times m$ identity matrix as $I_{m \times m}$ for any positive integer m . We employ $\|x\|_q$ to represent the l_q norm of any vector x . For any matrix X , X' denotes its transpose, $\|X\|$ and $\|X\|_F$ represent the spectral and Frobenius norms, respectively, $\text{rank}(X)$ denotes its rank, $X(i, :)$ indicates its i -th row, and $\lambda_k(X)$ stands for its k -th largest eigenvalue in magnitude. Additionally, $\mathbb{E}[\cdot]$ and $\mathbb{P}(\cdot)$ are used to represent expectation and probability, respectively.

2. The multi-layer degree-corrected stochastic co-block model

Consider a multi-layer bipartite network, denoted as \mathcal{N} , composed of L distinct layers. This network possesses n_r common row nodes and n_c common column nodes. Specifically, \mathcal{N}_l represents the bipartite network situated in the l -th layer for $l \in [L]$. For each bipartite network \mathcal{N}_l within the multi-layer structure, an adjacency matrix A_l is defined, which belongs to the set $\{0, 1\}^{n_r \times n_c}$. This matrix serves as a comprehensive record of the connectivity patterns between row and column nodes. Precisely, $A_l(i_r, j_c)$ is assigned a value of 1 whenever a directed edge exists from row node (sending node) i_r to column node (receiving node) j_c , and it is set to 0 in the absence of such an edge for

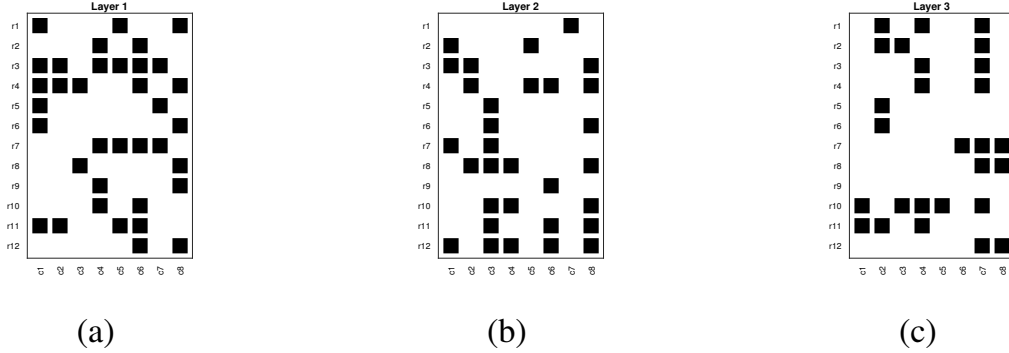


Figure 3: The adjacency matrices corresponding to the 3 distinct layers of the multi-layer bipartite network shown in Figure 2, where black square represents 1.

$i_r \in [n_r], j_c \in [n_c], l \in [L]$. Here, the subscript “r” represents rows, and the subscript “c” denotes columns. Figure 3 shows the adjacency matrices corresponding to the three layers of the multi-layer bipartite network displayed in Figure 2. It is noteworthy that when the set of row nodes coincides with the set of column nodes, the bipartite network \mathcal{N} simplifies to a multi-layer directed network. Furthermore, in the special case where the set of row nodes coincides with the set of column nodes and all edges are undirected, \mathcal{N} reduces to a multi-layer undirected network.

Suppose that all layers share a common row community structure and a common column community structure. Specifically, all row nodes belong to K_r disjoint row communities, denoted as $\{C_{r,1}, C_{r,2}, \dots, C_{r,K_r}\}$, while all column nodes belong to K_c disjoint column communities, represented as $\{C_{c,1}, C_{c,2}, \dots, C_{c,K_c}\}$. Here, C_{r,k_r} is a collection of row nodes belonging to the k_r -th row community for $k_r \in [K_r]$ and C_{c,k_c} is a collection of column nodes belonging to the k_c -th column community for $k_c \in [K_c]$. We assume that the number of row communities K_r and the number of column communities K_c are known in this paper.

Let Z_r be an $n_r \times K_r$ matrix, with entries in $\{0, 1\}$, representing the common row membership matrix of row nodes. Specifically, $Z_r(i_r, k_r) = 1$ if the row node i_r belongs to the k_r -th row community, C_{r,k_r} , and 0 otherwise, for each $i_r \in [n_r]$. Since we assume mutual exclusivity among row communities, each row of Z_r features exactly one entry as 1, while the remaining $K_r - 1$ entries are zeros. Assuming that each row community encompasses at least one row node, we infer that the rank of Z_r is K_r . Analogously, let Z_c be an $n_c \times K_c$ matrix, also with entries in $\{0, 1\}$, serving as the common column membership matrix of column nodes. Here, $Z_c(j_c, k_c) = 1$ if the column node j_c belongs to the k_c -th column community, and 0 otherwise, for each $j_c \in [n_c]$. Similar to Z_r , each row of Z_c contains exactly one 1, with the remaining entries as zeros, and the rank of Z_c is K_c .

Let θ_r be an $n_r \times 1$ vector such that $\theta_r(i_r)$ is the common degree heterogeneity shared by all layers of row node i_r and $\theta_r(i_r) \in (0, 1]$ for $i_r \in [n_r]$. Similarly, let $\theta_c \in (0, 1]^{n_c \times 1}$ be the common degree heterogeneity vector shared by all layers of column nodes. Define Θ_r as an $n_r \times n_r$ diagonal matrix and Θ_c as an $n_c \times n_c$ diagonal matrix such that $\Theta_r(i_r, i_r) = \theta_r(i_r)$ for each $i_r \in [n_r]$, and $\Theta_c(j_c, j_c) = \theta_c(j_c)$ for each $j_c \in [n_c]$.

Let B_l represent a $K_r \times K_c$ asymmetric matrix such that $B_l \in [0, 1]^{K_r \times K_c}$ for $l \in [L]$. We refer to B_l as the block connectivity matrix. Given the row community classification matrix Z_r , the column community classification matrix Z_c , along with the row degree heterogeneity vector θ_r and the column degree heterogeneity vector θ_c , as well as the L block connectivity matrices $\{B_l\}_{l=1}^L$, we assume that the adjacency matrix for each layer of the multi-layer bipartite network \mathcal{N} is generated by the degree-corrected stochastic co-block model (Rohe et al., 2016). To be precise, to model a multi-layer bipartite network with true row membership matrix Z_r and true column membership matrix Z_c , we consider the following model, which is a multi-layer version of DC-ScBM.

Definition 1. (Multi-layer DC-ScBM) Let $A_l \in \{0, 1\}^{n_r \times n_c}$ be the adjacency matrix of the l -th layer bipartite network \mathcal{N}_l , $Z_r \in \mathbb{M}_{n_r, K_r}$ be the common row membership matrix, $Z_c \in \mathbb{M}_{n_c, K_c}$ be the common column membership matrix, $\theta_r \in (0, 1]^{n_r \times 1}$ be the common row degree heterogeneity vector, $\theta_c \in (0, 1]^{n_c \times 1}$ be the common column degree heterogeneity vector, and $B_l \in [0, 1]^{K_r \times K_c}$ be the l -th block connectivity matrix for $l \in [L]$. Our multi-layer DC-ScBM assumes that

for each pair (i_r, j_c) (with $i_r \in [n_r]$ and $j_c \in [n_c]$) and each layer $l \in [L]$, $A_l(i_r, j_c)$ are independently generated from a Bernoulli distribution such that

$$A_l(i_r, j_c) \sim \text{Bernoulli}(\Omega_l(i_r, j_c)), \text{ where } \Omega_l := \Theta_r Z_r B_l Z_c' \Theta_c. \quad (1)$$

By Equation (1), we see that $\mathbb{E}[A_l] = \Omega_l$ for $l \in [L]$ under the multi-layer DC-ScBM. Meanwhile, Equation (1) gives that $\mathbb{P}(A_l(i_r, j_c) = 1) = \theta_r(i_r)\theta_c(j_c)Z_r(i_r, :)B_l Z_c'(j_c, :)$ for $i_r \in [n_r], j_c \in [n_c], l \in [L]$ under the multi-layer DC-ScBM, which implies that the probability of generating an edge from row node i_r to column node j_c does not only depend on their belonging communities but also relies on their unique characteristics through the degree heterogeneity parameters $\theta_r(i_r)$ and $\theta_c(j_c)$. Equation (1) also specifies that the multi-layer DC-ScBM is parameterized by $(Z_r, Z_c, \Theta_r, \Theta_c, \{B_l\}_{l=1}^L)$. Suppose that A_1, A_2, \dots, A_L are generated from the multi-layer DC-ScBM according to Equation (1), the primary task of community detection in multi-layer bipartite networks is to recover the row membership matrix Z_r and the column membership matrix Z_c .

Our multi-layer DC-ScBM includes several previous network models as special cases. For example, when all entries of θ_r (and θ_c) are equal and all row nodes are the same as column nodes, our multi-layer DC-ScBM reduces to the multi-layer ScBM studied in (Su et al., 2023). When $Z_r = Z_c, \Theta_r = \Theta_c$, and B_l is symmetric for $l \in [L]$ such that \mathcal{N} is undirected, and all entries of θ_r are equal, our multi-layer DC-ScBM degenerates to the popular multi-layer SBM considered in (Han et al., 2015; Paul & Chen, 2016, 2020; Lei et al., 2020; Lei & Lin, 2023). When $L = 1$, the multi-layer DC-ScBM reduces to the DC-ScBM (Rohe et al., 2016). When $L = 1$ and all entries of θ_r (and θ_c) are the same, the multi-layer DC-ScBM reduces to the ScBM (Rohe et al., 2016). When $L = 1$ and \mathcal{N} is undirected, the multi-layer DC-ScBM degenerates to the well-known DCSBM (Karrer & Newman, 2011). Furthermore, if all entries of the degree heterogeneity vector are the same, the multi-layer DC-ScBM degenerates to the well-known SBM (Holland et al., 1983).

3. Algorithm

In this section, we describe one community detection algorithm to efficiently detect both row and column communities for multi-layer bipartite networks generated from the multi-layer DC-ScBM. The following lemma is the cornerstone of our algorithm.

Lemma 1. Consider the multi-layer DC-ScBM parameterized by $(Z_r, Z_c, \Theta_r, \Theta_c, \{B_l\}_{l=1}^L)$.

- Suppose that $\text{rank}(\sum_{l \in [L]} B_l B_l') = K$, where $K \leq K_r$. Set $\tilde{S}_r = \sum_{l \in [L]} \Omega_l \Omega_l'$. Let $U_r \Lambda_r U_r'$ be the top K eigen-decomposition of \tilde{S}_r such that $U_r' U_r = I_{K \times K}$ and Λ_r is a $K \times K$ diagonal matrix with k -th diagonal element being the k -th largest eigenvalue in magnitude of \tilde{S}_r for $k \in [K]$. Let U_r^* be the row-normalized version of U_r such that $U_r^*(i_r, :) = \frac{U_r(i_r, :)}{\|U_r(i_r, :)\|_F}$ for $i_r \in [n_r]$. Then $U_r^*(i_r, :) = U_r^*(\tilde{i}_r, :)$ if and only if $Z_r(i_r, :) = Z_r(\tilde{i}_r, :)$ for $i_r \in [n_r], \tilde{i}_r \in [n_r]$. Furthermore, when $K = K_r$, we have $\|U_r^*(i_r, :) - U_r^*(\tilde{i}_r, :)\|_F = \sqrt{2}$ for any two row nodes satisfying $Z_r(i_r, :) \neq Z_r(\tilde{i}_r, :)$.
- Suppose that $\text{rank}(\sum_{l \in [L]} B_l' B_l) = \tilde{K}$, where $\tilde{K} \leq K_c$. Set $\tilde{S}_c = \sum_{l \in [L]} \Omega_l' \Omega_l$. Let $U_c \Lambda_c U_c'$ be the top \tilde{K} eigen-decomposition of \tilde{S}_c such that $U_c' U_c = I_{\tilde{K} \times \tilde{K}}$ and Λ_c is a $\tilde{K} \times \tilde{K}$ diagonal matrix with \tilde{k} -th diagonal element being the \tilde{k} -th largest eigenvalue in magnitude of \tilde{S}_c for $\tilde{k} \in [\tilde{K}]$. Let U_c^* be the row-normalized version of U_c such that $U_c^*(j_c, :) = \frac{U_c(j_c, :)}{\|U_c(j_c, :)\|_F}$ for $j_c \in [n_c]$. Then $U_c^*(j_c, :) = U_c^*(\tilde{j}_c, :)$ if and only if $Z_c(j_c, :) = Z_c(\tilde{j}_c, :)$ for $j_c \in [n_c], \tilde{j}_c \in [n_c]$. Furthermore, when $\tilde{K} = K_c$, we have $\|U_c^*(j_c, :) - U_c^*(\tilde{j}_c, :)\|_F = \sqrt{2}$ for any two column nodes satisfying $Z_c(j_c, :) \neq Z_c(\tilde{j}_c, :)$.

By Lemma 1, it becomes evident that U_r^* possesses precisely K_r unique rows. This observation suggests that by implementing the K-means algorithm on all rows of U_r^* with K_r clusters, we can accurately identify the row communities. Analogously, applying the K-means algorithm to all rows of U_c^* with K_c clusters will precisely reveal the column communities. To streamline our analysis, we will concentrate on the scenario where both $\sum_{l \in [L]} B_l B_l'$ and $\sum_{l \in [L]} B_l' B_l$ are of full rank, thereby implying $K = K_r$ and $\tilde{K} = K_c$. Consequently, the l_2 norm of the difference between any two distinct rows of U_r^* (and similarly, U_c^*) equals $\sqrt{2}$.

Set $S_r = \sum_{l \in [L]} (A_l A_l' - D_l^r)$, where D_l^r is an $n_r \times n_r$ diagonal matrix with i_r -th diagonal element being $\sum_{j_c \in [n_c]} A_l(i_r, j_c)$ for $i_r \in [n_r], l \in [L]$. Set $S_c = \sum_{l \in [L]} (A_l' A_l - D_l^c)$, where D_l^c is an $n_c \times n_c$ diagonal matrix with j_c -th diagonal element being $\sum_{i_r \in [n_r]} A_l(i_r, j_c)$ for $j_c \in [n_c], l \in [L]$. According to the analysis in (Lei & Lin, 2023; Su et al., 2023), S_r and S_c serve as debiased estimations of \tilde{S}_r and \tilde{S}_c , respectively, whereas $\sum_{l \in [L]} A_l A_l'$ and $\sum_{l \in [L]} A_l' A_l$ are biased estimates of \tilde{S}_r and \tilde{S}_c , respectively. Let $\hat{U}_r \hat{\Lambda}_r \hat{U}_r'$ be the top K_r eigen-decomposition of S_r such that $\hat{U}_r' \hat{U}_r = I_{K_r \times K_r}$ and $\hat{\Lambda}_r$ is a $K_r \times K_r$ diagonal matrix with k_r -th diagonal entry being the k_r -th largest eigenvalue in magnitude of S_r for $k_r \in [K_r]$. Let \hat{U}_r^* be the row-normalized version of \hat{U}_r such that $\hat{U}_r^*(i_r, :) = \frac{\hat{U}_r(i_r, :)}{\|\hat{U}_r(i_r, :)\|_F}$ for $i_r \in [n_r]$. Since S_r is a debiased estimate of \tilde{S}_r , \hat{U}_r^* is a good approximation of U_r^* and it should have roughly K_r distinct rows. Consequently, applying the K-means algorithm to all rows of \hat{U}_r^* should return a good estimation of row communities. Similarly, letting $\hat{U}_c \hat{\Lambda}_c \hat{U}_c'$ be the top K_c eigen-decomposition of S_c and \hat{U}_c^* be the row-normalized version of \hat{U}_c , applying K-means algorithm to all rows of \hat{U}_c^* should provide an accurate estimation of column communities. The following four-stage algorithm which we call NcDSoS summarizes the above analysis.

Algorithm 1 Normalized spectral co-clustering based on debiased sum of squared matrices (NcDSoS)

Require: Adjacency matrices A_1, A_2, \dots, A_L , number of row communities K_r , and number of column communities K_c , where $A_l \in \{0, 1\}^{n_r \times n_c}$ for $l \in [L]$.

Ensure: Estimated row membership matrix $\hat{Z}_r \in \mathbb{M}_{n_r, K_r}$ and estimated column membership matrix $\hat{Z}_c \in \mathbb{M}_{n_c, K_c}$.

- 1: Compute $S_r = \sum_{l \in [L]} (A_l A_l' - D_l^r)$ and $S_c = \sum_{l \in [L]} (A_l' A_l - D_l^c)$.
 - 2: Compute the $n_r \times K_r$ matrix \hat{U}_r containing the top K_r eigenvectors (ordered in absolute eigenvalue) of S_r and the $n_c \times K_c$ matrix \hat{U}_c containing the top K_c eigenvectors (ordered in absolute eigenvalue) of S_c .
 - 3: Compute \hat{U}_r^* and \hat{U}_c^* by normalizing each row of \hat{U}_r and \hat{U}_c to have unit length, respectively.
 - 4: Run K-means algorithm on rows of \hat{U}_r^* with K_r clusters to obtain the estimated row membership matrix \hat{Z}_r and run K-means algorithm on rows of \hat{U}_c^* with K_c clusters to obtain the estimated column membership matrix \hat{Z}_c .
-

4. Theoretical properties

We consider the *Clustering error* introduced in (Joseph & Yu, 2016) to evaluate the performance of a community detection algorithm when the true row and column membership matrices are available. For $k_r \in [K_r]$, let \hat{C}_{r, k_r} be the estimated k_r -th row community, i.e., $\hat{C}_{r, k_r} = \{i \in [n_r] : \hat{Z}_r(i, k_r) = 1\}$. For $k_c \in [K_c]$, let \hat{C}_{c, k_c} be the estimated k_c -th column community, i.e., $\hat{C}_{c, k_c} = \{j \in [n_c] : \hat{Z}_c(j, k_c) = 1\}$. The clustering errors for row communities and column communities are defined as

$$\begin{aligned} \hat{f}_r &= \min_{\pi \in S_{K_r}} \max_{k_r \in [K_r]} (|C_{r, k_r} \cap \hat{C}_{r, \pi(k_r)}^c| + |C_{r, k_r}^c \cap \hat{C}_{r, \pi(k_r)}|) / n_{r, k_r}, \\ \hat{f}_c &= \min_{\pi \in S_{K_c}} \max_{k_c \in [K_c]} (|C_{c, k_c} \cap \hat{C}_{c, \pi(k_c)}^c| + |C_{c, k_c}^c \cap \hat{C}_{c, \pi(k_c)}|) / n_{c, k_c}, \end{aligned}$$

where n_{r, k_r} is the number of row nodes belonging to the k_r -th row community, n_{c, k_c} is the number of column nodes belonging to the k_c -th column community, S_{K_r} is the set of all permutations of $\{1, 2, \dots, K_r\}$, S_{K_c} is the set of all permutations of $\{1, 2, \dots, K_c\}$, and the superscript c represents a complementary set.

Our main theoretical result provides upper bounds on Clustering errors \hat{f}_r and \hat{f}_c for both row and column nodes. To establish our theoretical guarantees, we need the following assumption to control the overall sparsity of the multi-layer bipartite network \mathcal{N} .

Assumption 1. $\min(\theta_{r, \max} \|\theta_r\|_1 \|\theta_c\|_F^2, \theta_{c, \max} \|\theta_c\|_1 \|\theta_r\|_F^2) \geq \frac{\log(n_r + n_c + L)}{L}$, where $\theta_{r, \max} = \max_{i \in [n_r]} \theta_r(i)$ and $\theta_{c, \max} = \max_{j \in [n_c]} \theta_c(j)$.

At first glance, Assumption 1 might be complex. To gain a deeper understanding, let's consider a particular scenario where we set $n_r = n_c = n$, $\Theta_r = \Theta_c = \sqrt{\rho} I_{n \times n}$ for $\rho \in (0, 1]$. For this case, Assumption 1 simplifies to the more straightforward form $\rho n \geq \frac{\log(2n+L)}{L}$. Essentially, this indicates that the sparsity parameter ρ should decrease at a rate slower than $\frac{\log(2n+L)}{L}$, which is a relatively weak requirement for ρ . Meanwhile, this also underscores the benefit of exploring multi-layer networks for community detection as increasing the number of layers L decreases the lower bound requirement on the network's sparsity. Furthermore, when our multi-layer DC-ScBM degenerates to the

multi-layer SBM, the assumption $\rho n \geq \frac{\log(2n+L)}{L} > \frac{\log(n+L)}{L}$ is consistent with the sparsity requirement in Theorem 1 of (Lei & Lin, 2023) under the multi-layer SBM model. This guarantees the optimality of our sparsity requirement in Assumption 1.

The lemma below precisely quantifies the spectral norm of $\|S_r - \tilde{S}_r\|$ and $\|S_c - \tilde{S}_c\|$. In the core of the analysis, we take advantage of the rectangular case of matrix Bernstein inequality (Tropp, 2012).

Lemma 2. *For the multi-layer DC-ScBM parameterized by $(Z_r, Z_c, \Theta_r, \Theta_c, \{B_l\}_{l=1}^L)$, suppose Assumption 1 holds, with probability at least $1 - o(\frac{1}{n_r+n_c+L})$, we have*

$$\begin{aligned}\|S_r - \tilde{S}_r\| &= O\left(\sqrt{\theta_{r,\max}\|\theta_r\|_1\|\theta_c\|_F^2 L \log(n_r + n_c + L)}\right) + O(\theta_{r,\max}^2\|\theta_c\|_F^2 L), \\ \|S_c - \tilde{S}_c\| &= O\left(\sqrt{\theta_{c,\max}\|\theta_c\|_1\|\theta_r\|_F^2 L \log(n_r + n_c + L)}\right) + O(\theta_{c,\max}^2\|\theta_r\|_F^2 L).\end{aligned}$$

For our theoretical analysis, we need to pose conditions on the block connectivity matrices $\{B_l\}_{l=1}^L$. The following assumption requires a linear growth of $|\lambda_{K_r}(\sum_{l \in [L]} B_l B_l')|$ and $|\lambda_{K_c}(\sum_{l \in [L]} B_l' B_l)|$ when the number of layers L increases.

Assumption 2. $|\lambda_{K_r}(\sum_{l \in [L]} B_l B_l')| \geq c_1 L$ and $|\lambda_{K_c}(\sum_{l \in [L]} B_l' B_l)| \geq c_2 L$ for some constants $c_1 > 0$ and $c_2 > 0$.

Remark 1. Here, we explain why conditions in Assumption 2 are mild. Note that B_l is a $K_r \times K_c$ matrix, Assumption 2 does not require each B_l being full rank but only requires $\sum_{l \in [L]} B_l B_l'$ and $\sum_{l \in [L]} B_l' B_l$ being full rank.

The following theorem represents our primary theoretical finding for the proposed NcDSoS approach. It establishes upper bounds for the clustering error of both row and column communities, expressed in terms of various model parameters, within the context of the multi-layer DC-ScBM model.

Theorem 1. *Let \hat{Z}_r and \hat{Z}_c be obtained from Step 4 of Algorithm 1. For the multi-layer DC-ScBM parameterized by $(Z_r, Z_c, \Theta_r, \Theta_c, \{B_l\}_{l=1}^L)$, when Assumptions 1 and 2 hold, with probability at least $1 - o(\frac{1}{n_r+n_c+L})$, we have*

$$\begin{aligned}\hat{f}_r &= O\left(\frac{\theta_{r,\max}^3 K_r^2 n_{r,\max} \|\theta_r\|_1 \|\theta_c\|_F^2 \log(n_r + n_c + L)}{\theta_{r,\min}^6 \theta_{c,\min}^4 n_{r,\min}^3 n_{c,\min}^2 L}\right) + O\left(\frac{\theta_{r,\max}^6 K_r^2 n_{r,\max} \|\theta_c\|_F^4}{\theta_{r,\min}^6 \theta_{c,\min}^4 n_{r,\min}^3 n_{c,\min}^2}\right) \\ \hat{f}_c &= O\left(\frac{\theta_{c,\max}^3 K_c^2 n_{c,\max} \|\theta_c\|_1 \|\theta_r\|_F^2 \log(n_r + n_c + L)}{\theta_{r,\min}^4 \theta_{c,\min}^6 n_{r,\min}^2 n_{c,\min}^3 L}\right) + O\left(\frac{\theta_{c,\max}^6 K_c^2 n_{c,\max} \|\theta_r\|_F^4}{\theta_{r,\min}^4 \theta_{c,\min}^6 n_{r,\min}^2 n_{c,\min}^3}\right).\end{aligned}$$

where $\theta_{r,\min} = \min_{i \in [n_r]} \theta_r(i)$, $\theta_{c,\min} = \min_{j \in [n_c]} \theta_c(j)$, $n_{r,\max} = \max_{k_r \in [K_r]} n_{r,k_r}$, $n_{r,\min} = \min_{k_r \in [K_r]} n_{r,k_r}$, $n_{c,\max} = \max_{k_c \in [K_c]} n_{c,k_c}$, and $n_{c,\min} = \min_{k_c \in [K_c]} n_{c,k_c}$.

Theorem 1 underscores the enhanced accuracy of community partitions obtained from NcDSoS as the number of layers, L , increases. This finding underscores the advantage of incorporating multiple layers in community detection tasks. Conversely, Theorem 1 also indicates that a reduction in the size of the smallest row (and column) communities leads to increased error rates. Although Theorem 1 is stated in a rather complex manner, involving numerous model parameters, the subsequent corollary simplifies its complexity by imposing certain conditions on these parameters.

Corollary 1. *Under the same conditions of Theorem 1, when $K_r = O(1)$, $K_c = O(1)$, $\frac{n_{r,\min}}{n_{r,\max}} = O(1)$, $\frac{n_{c,\min}}{n_{c,\max}} = O(1)$, $\theta_{r,\min} = O(\sqrt{\rho})$, $\theta_{r,\max} = O(\sqrt{\rho})$, $\theta_{c,\min} = O(\sqrt{\rho})$, and $\theta_{c,\max} = O(\sqrt{\rho})$ for $\rho \in (0, 1]$, we have*

$$\hat{f}_r = O\left(\frac{\log(n_r + n_c + L)}{\rho^2 n_r n_c L}\right) + O\left(\frac{1}{n_r^2}\right) \text{ and } \hat{f}_c = O\left(\frac{\log(n_r + n_c + L)}{\rho^2 n_r n_c L}\right) + O\left(\frac{1}{n_c^2}\right).$$

If we further assume that $n_r = O(n_c) = O(n)$, we have

$$\hat{f}_r = \hat{f}_c = O\left(\frac{\log(n+L)}{\rho^2 n^2 L}\right) + O\left(\frac{1}{n^2}\right).$$

In Corollary 1, the condition $n_{r,\min}/n_{r,\max} = O(1)$ ensures that the sizes of row communities remain balanced. According to this corollary, to achieve sufficiently low error rates, the sparsity parameter ρ should decrease slower than $\sqrt{\frac{\log(n_r+n_c+L)}{n_r n_c L}}$, which aligns precisely with Assumption 1. Meanwhile, increasing the sparsity parameter ρ decreases the error rates. Furthermore, Corollary 1 demonstrates that as the number of row (or column) nodes and/or the number of layers increases to infinity, the error rates of NcDSoS converge to zero, thus establishing its consistency. Additionally, when we set $Z_r = Z_c$, $n_r = n_c = n$, $\Theta_r = \Theta_c = \sqrt{\rho}I_{n \times n}$ for $\rho \in (0, 1]$, and $B_l = B'_l$ for $l \in [L]$, our multi-layer DC-ScBM simplifies to the multi-layer SBM. In this case, the theoretical upper bounds of error rates derived for NcDSoS align with the theoretical results presented in Theorem 1 of Lei & Lin (2023), indicating the optimality of our theoretical analysis.

5. Simulations

In this section, we investigate the empirical performance of NcDSoS for detecting communities of the multi-layer DC-ScBM model by comparing it with the following algorithms:

- **NcSoS**: Normalized spectral co-clustering based on sum of squared matrices. NcSoS uses the non-debiased matrices $\sum_{l \in [L]} A_l A'_l$ and $\sum_{l \in [L]} A'_l A_l$ to replace S_r and S_c in Algorithm 1. Since $\|\sum_{l \in [L]} A_l A'_l - \tilde{S}_r\| = \|S_r - \tilde{S}_r + \sum_{l \in [L]} D_l^r\| \leq \|S_r - \tilde{S}_r\| + \|\sum_{l \in [L]} D_l^r\|$ and $\|\sum_{l \in [L]} A'_l A_l - \tilde{S}_c\| = \|S_c - \tilde{S}_c + \sum_{l \in [L]} D_l^c\| \leq \|S_c - \tilde{S}_c\| + \|\sum_{l \in [L]} D_l^c\|$, following a similar proof of Theorem 1, we can immediately build NcSoS's theoretical guarantees and find that the theoretical upper bounds of NcSoS's clustering errors are larger than that of NcDSoS. This analysis underscores the importance of debiasing in enhancing the performance of spectral co-clustering methods for community detection in multi-layer bipartite networks.
- **NcSum**: Normalized spectral co-clustering based on sum of adjacency matrices. NcSum detects row (and column) communities by employing the K-means algorithm on the row-normalized version of the top $\min(K_r, K_c)$ left (and right) singular vectors of $\sum_{l \in [L]} A_l$ with K_r (and K_c) clusters.
- **Sum**: this algorithm is proposed in (Su et al., 2023) and it detects row (and column) communities by running the K-means algorithm on the top $\min(K_r, K_c)$ left (and right) singular vectors of $\sum_{l \in [L]} A_l$ with K_r (and K_c) clusters.
- **SoG**: this method introduced in (Su et al., 2023) estimates row (and column) communities by running K-means algorithm on the eigenvectors of the non-debiased matrix $\sum_{l \in [L]} A_l A'_l$ (and $\sum_{l \in [L]} A'_l A_l$) with K_r (and K_c) clusters.
- **DSoG**: this method proposed in (Su et al., 2023) estimates row (and column) communities by running K-means algorithm on the eigenvectors of S_r (and S_c) with K_r (and K_c) clusters.

To assess the performance of the aforementioned algorithms, we employ four evaluation metrics: Clustering error, Hamming error (Jin, 2015), normalized mutual information (NMI) (Strehl & Ghosh, 2002; Danon et al., 2005; Bagrow, 2008), and adjusted rand index (ARI) (Hubert & Arabie, 1985; Vinh et al., 2009). The details of these metrics are given below::

- **Clustering error**: In our simulation studies, we define Clustering error as $\max(\hat{f}_r, \hat{f}_c)$ to simplify our analysis. This metric is non-negative, and a lower value indicates better performance in community detection for both row and column communities.
- **Hamming error**: This metric quantifies the similarity between the predicted and actual community assignments. It is defined as $\max(\min_{P_r \in \mathcal{P}_{K_r}} \|\hat{Z}_r P_r - Z_r\|_0 / n_r, \min_{P_c \in \mathcal{P}_{K_c}} \|\hat{Z}_c P_c - Z_c\|_0 / n_c)$ where \mathcal{P}_{K_r} (and \mathcal{P}_{K_c}) represents the set of all $K_r \times K_r$ (and $K_c \times K_c$) permutation matrices. The Hamming error ranges from 0 to 1, with a lower value indicating better performance.
- **NMI and ARI**: We adopt the NMI and ARI definitions from (Qing & Wang, 2023) to assess the quality of community detection in both row and column communities. NMI ranges from 0 to 1, while ARI ranges from -1 to 1. In both cases, a higher value indicates better performance.

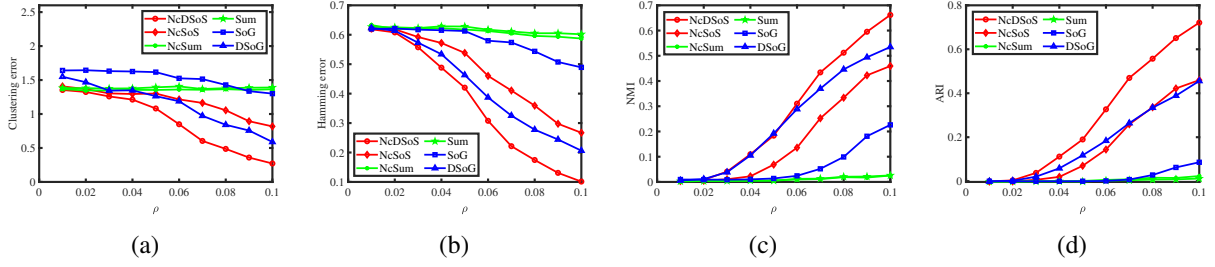


Figure 4: Experiment 1. Panel (a): Clustering error against increasing ρ . Panel (b): Hamming error against increasing ρ . Panel (c): NMI against increasing ρ . Panel (d): ARI against increasing ρ .

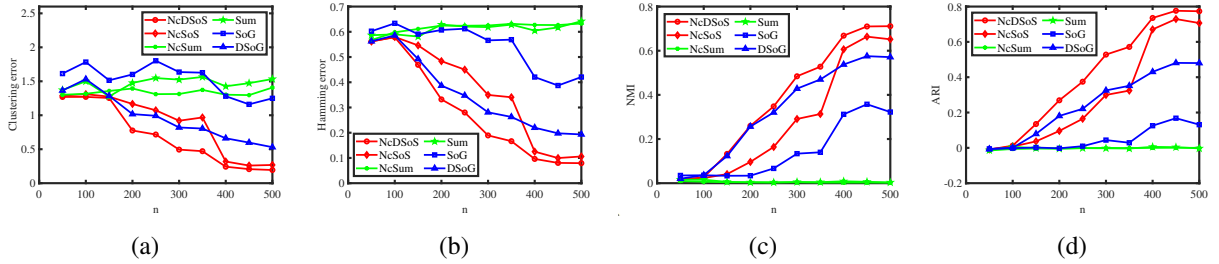


Figure 5: Experiment 2. Panel (a): Clustering error against increasing n . Panel (b): Hamming error against increasing n . Panel (c): NMI against increasing n . Panel (d): ARI against increasing n .

By leveraging these metrics, we can comprehensively evaluate the performance of the algorithms in community detection tasks.

In all simulated multi-layer bipartite networks, we consistently assign $K_r = 2$ and $K_c = 3$ as fixed parameters. Subsequently, we generate Z_r and Z_c in a manner that ensures that each row (and column) node belongs to each row (and column) community with an equivalent probability. For $i \in [n_r]$ and $j \in [n_c]$, we set $\theta_r(i) = \sqrt{\rho} \cdot \text{rand}(1)$ and $\theta_c(j) = \sqrt{\rho} \cdot \text{rand}(1)$, respectively, where $\text{rand}(1)$ represents a random value drawn from the uniform distribution on the interval $(0, 1)$. Furthermore, we assign $B_l(k_r, k_c) = \text{rand}(1)$ for $k_r \in [K_r], k_c \in [K_c]$, and $l \in [L]$. The four parameters n_r, n_c, L , and ρ are set independently for each experiment. Notably, in Experiment 2, where we specifically consider the case where n_r equals n_c , we simplify the notation by setting $n = n_r = n_c$ for convenience. To ensure reliability and reproducibility, we report each metric for different methods, averaging the results over 100 random runs for each parameter setting.

Experiment 1: Changing ρ . We set $n_r = 200, n_c = 300, L = 50$, and let ρ range in $\{0.01, 0.02, 0.03, \dots, 0.1\}$. Based on the results shown in Figure 4, we have the following observations: (a) Our method NcDSoS significantly outperforms its competitors. (b) The performance of NcDSoS improves as the sparsity parameter ρ increases, aligning with our theoretical predictions. (c) Although both NcDSoS and DSoG incorporate debiased spectral clustering, NcDSoS surpasses DSoG because NcDSoS is designed to fit the multi-layer DC-ScBM while DSoG is for the multi-layer ScBM and our multi-layer DC-ScBM considers the degree heterogeneity of nodes while the multi-layer ScBM does not. Similar arguments hold for NcSum and SoG.

Experiment 2: Changing n . We set $L = 20, \rho = 0.1, n_r = n_c = n$, and increase n from 50 to 500. Figure 5 displays the results. We see that (a) our NcDSoS outperforms the other five algorithms; (b) NcDSoS performs better when n increases and this is consistent with our theoretical results.

Experiment 3: Changing L . We set $n_r = 500, n_c = 600, \rho = 0.1$, and let L range in $\{5, 10, 15, \dots, 50\}$. Figure 6 shows the results. The data indicates that our NcDSoS outperforms its competitors across all parameter settings. Furthermore, NcDSoS exhibits better performance as the number of layers increases, aligning with our theoretical analysis.

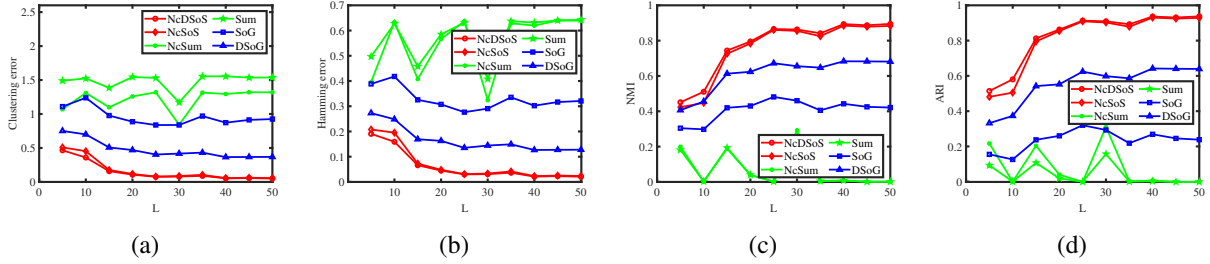


Figure 6: Experiment 3. Panel (a): Clustering error against increasing L . Panel (b): Hamming error against increasing L . Panel (c): NMI against increasing L . Panel (d): ARI against increasing L .

6. Real data applications

In this section, we consider the following real-world multi-layer directed networks, which can be downloaded from <https://manliodedomenico.com/data.php>:

- **Vickers Chan 7thGraders** : This data was collected by Vickers from 29 seventh grade students in a school in Victoria, Australia. Students were asked to nominate their classmates on three interpersonal relations (layers): Who do you get on with in the class? Who are your best friends in the class? Who would you prefer to work with?
- **Lazega law firm**: This data encompasses three distinct types of interactions: Co-work, Friendship, and Advice, occurring among partners and associates within a corporate law partnership.
- **C.elegans**: This data encompasses distinct layers that correspond to varying synaptic junctions. These layers include electric synaptic junctions ("ElectrJ"), chemical monadic synapses ("MonoSyn"), and chemical polyadic synapses ("PolySyn"), each capturing a unique aspect of neuronal connectivity within the *Caenorhabditis elegans*.

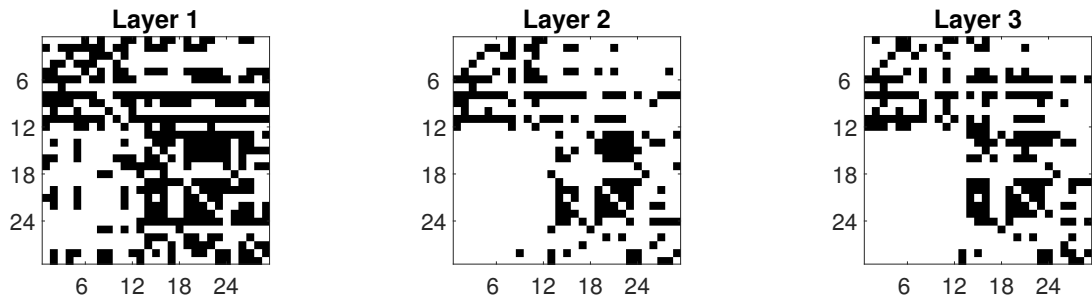
Figure 7 and Table 1 display the adjacency matrices and basic information of these real data sets, respectively. Notably, the adjacency matrices of Vickers Chan 7thGraders and Lazega law firm exhibit a pronounced asymmetry, indicating a significant divergence between their sending and receiving patterns. In contrast, the adjacency matrices of *C.elegans* display a near-symmetric pattern, suggesting a remarkable similarity in their sending and receiving behaviors.

Table 1: Basic information of real-world multi-layer directed networks used in this paper.

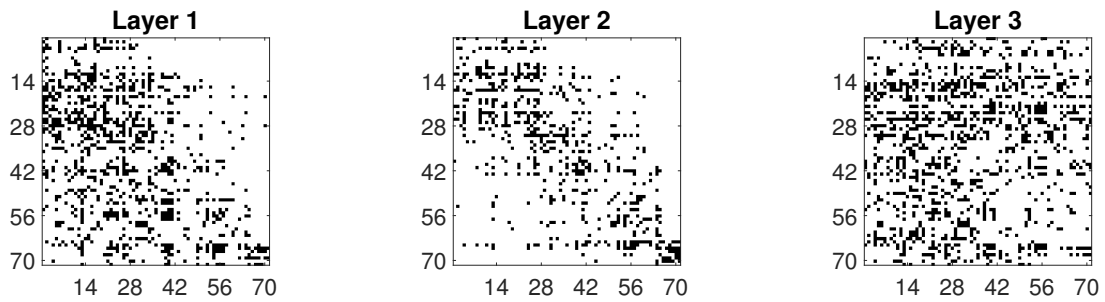
Dataset	Source	Directed?	# Nodes	# Layers	# Edges
Vickers Chan 7thGraders	(Vickers & Chan, 1981)	Yes	29	3	740
Lazega law firm	(Lazega, 2001; Sniijders et al., 2006)	Yes	71	3	2223
<i>C.elegans</i>	(Chen et al., 2006; De Domenico et al., 2015b)	Yes	279	3	5863

In any real-world multi-layer directed network comprising n nodes, we define two $n \times 1$ vectors, d_r^l and d_c^l , for each layer l in the range $[L]$. Specifically, $d_r^l(i)$ represents the out-degree of node i in layer l , calculated as the sum of all elements in the i^{th} row of the adjacency matrix A_l , i.e., $d_r^l(i) = \sum_{j \in [n]} A_l(i, j)$. Similarly, $d_c^l(i)$ represents the in-degree of node i in layer l , obtained by summing the elements in the i^{th} column of A_l , i.e., $d_c^l(i) = \sum_{j \in [n]} A_l(j, i)$. For brevity, we often refer to d_r^l and d_c^l simply as d_r and d_c when discussing any particular layer.

Figure 8 depicts the distributions of out-degree and in-degree in each layer, based on the real-world datasets utilized in this study. In the case of Vickers Chan's 7th Graders network, we observe significant variations in the distributions of in-degree and out-degree across layers, indicating a substantial difference in sending and receiving patterns. A similar trend is observed in the Lazega law firm network. However, for the *C.elegans* network, the



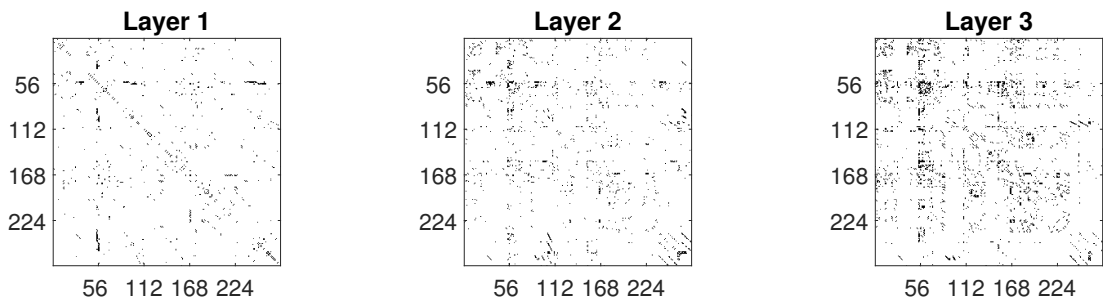
(a) Vickers Chan 7thGraders (b) Vickers Chan 7thGraders (c) Vickers Chan 7thGraders



(d) Lazega law firm

(e) Lazega law firm

(f) Lazega law firm



(g) C.elegans

(h) C.elegans

(i) C.elegans

Figure 7: The adjacency matrices of real multi-layer directed networks used in this paper. In all matrices, black represents 1 and white means 0.

distributions of in-degree and out-degree in each layer exhibit a considerable overlap, suggesting a similarity in the sending and receiving behaviors. These observations align perfectly with the insights gained from Figure 7.

When dealing with real-world multi-layer directed networks, we face a challenge as the ground-truth community memberships and the exact number of row (column) communities remain unknown. To simplify our analysis, we assume that the number of row communities (K_r) is equal to the number of column communities (K_c), denoted as K . To quantify the disparity between the row and column clusters, we employ four indices: Clustering error, Hamming error, Normalized Mutual Information (NMI), and Adjusted Rand Index (ARI). Each of these metrics is calculated based on the estimated row community assignments (\hat{Z}_r) and column community assignments (\hat{Z}_c). Figure 9 presents a graphical representation of how these four indices vary as K increases. Based on this analysis, we can draw the following conclusions:

- For Vickers Chan 7th Graders, the disparity between sending and receiving patterns is significant due to high Clustering and Hamming errors and low NMI and ARI values for \hat{Z}_r and \hat{Z}_c . This aligns with the distributions of in-degree and out-degree shown in Figure 8 panels (a)-(c). Notably, when $K = 3$, the Hamming error is minimized, and NMI and ARI are maximized, indicating a relatively close similarity between sending and receiving patterns for this data.
- In the case of the Lazega law firm, the sending pattern significantly differs from the receiving pattern, which concurs with the findings in Figure 8 panels (d)-(f). Notably, when $K = 2$, both Clustering and Hamming errors are minimized, while ARI attains its maximum, suggesting a close resemblance between the sending and receiving patterns for this value of K .
- For C.elegans, as displayed in the last three panels of Figure 8, the sending pattern closely resembles the receiving pattern. Furthermore, Figure 9 shows that for $K = 2$, Clustering and Hamming errors are minimal, while NMI and ARI are maximal. Considering this, along with the last three panels of Figure 8, $K = 2$ serves as an optimal choice for this data.

In our subsequent analysis, we specifically assign the value of K as 3 for Vickers Chan 7th Graders, 2 for the Lazega law firm, and 2 for C.elegans. This choice is made to maintain a relatively similar sending and receiving pattern within these datasets. Figure 10 presents a heatmap that visualizes the pairwise NMI scores among the six community detection methods for both the row and column communities of the three real-world multi-layer directed networks. The clustering outcomes vary among different community detection methods. Given that our NcDSoS has outperformed its competitors in previous simulations, we tend to believe that our approach yields more precise community partitions. For visualization purposes, Figures 11, 12, and 13 illustrate the estimated row and column communities derived from our proposed method for Vickers Chan 7thGraders, Lazega law firm, and C.elegans, respectively. Notably, we observe a significant divergence between the row and column communities in the Vickers Chan 7thGraders and Lazega law firm cases, whereas, for C.elegans, the row communities closely align with the column communities. These observations align well with our previous findings.

7. Conclusion

This paper addresses the challenge of community detection in multi-layer bipartite networks, a topic of significant importance in network science and data analysis. Unlike traditional multi-layer undirected networks, multi-layer bipartite networks consist of two distinct types of nodes, necessitating a specialized approach for community detection. To this end, we introduce a novel multi-layer degree-corrected stochastic co-block model (multi-layer DC-ScBM) that captures the latent community structure inherent in such networks. Our model extends previous network models by incorporating multi-layer bipartite networks and degree heterogeneity. We propose an efficient algorithm to detect communities within the proposed multi-layer DC-ScBM framework. The algorithm’s performance is guaranteed by a rigorous theoretical analysis, which provides upper bounds on clustering errors and highlights the benefits of leveraging additional layers of bipartite networks for improved accuracy in community detection. Our numerical experiments of both synthetic and real-world datasets demonstrate the superiority of our algorithm over existing methods. In summary, this paper makes a significant contribution to the field of network science by introducing a novel model and algorithm for community detection in multi-layer bipartite networks. Our work stands at the

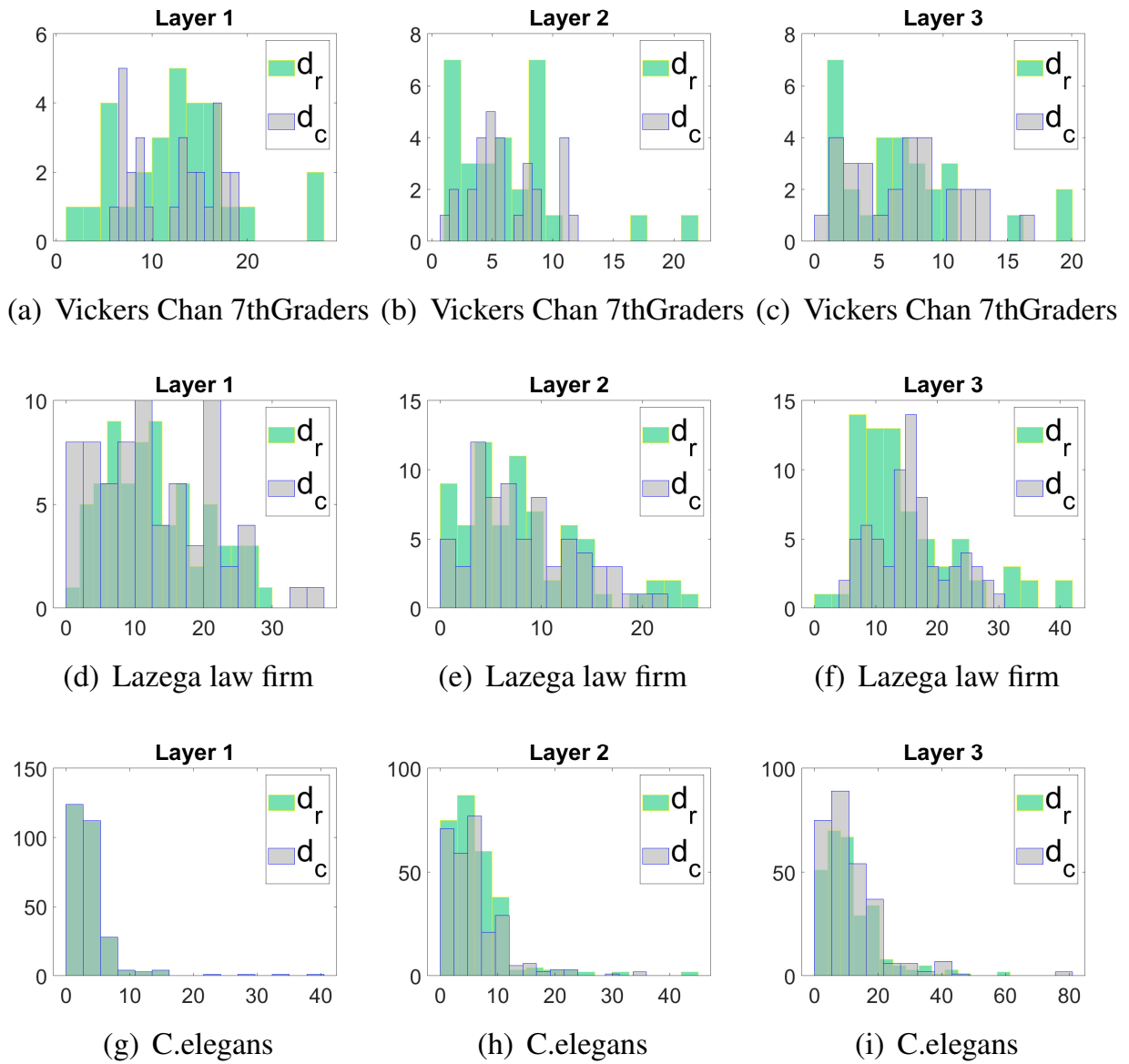
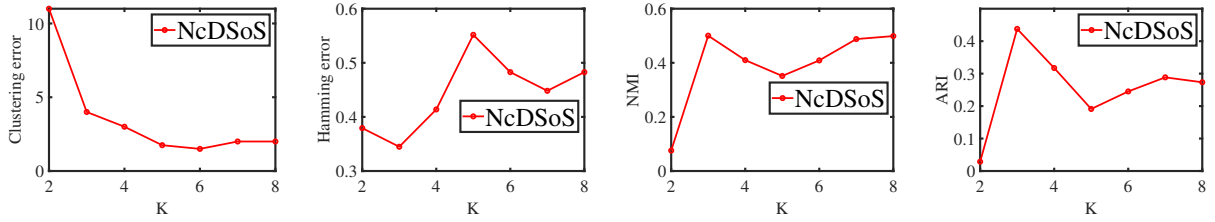
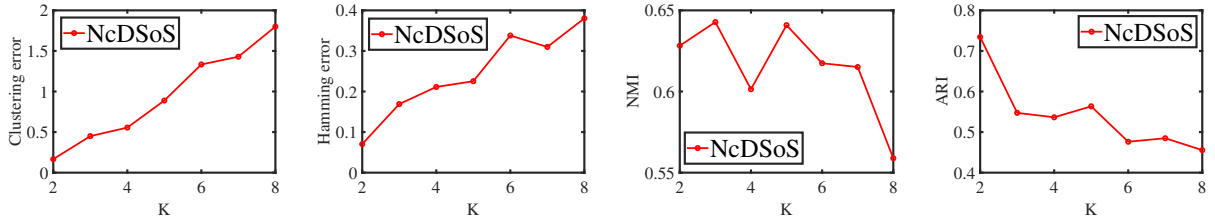


Figure 8: Distributions of d_r and d_c in each layer for real-world multi-layer directed networks considered in this paper.



(a) Vickers Chan 7thGraders (b) Vickers Chan 7thGraders (c) Vickers Chan 7thGraders (d) Vickers Chan 7thGraders

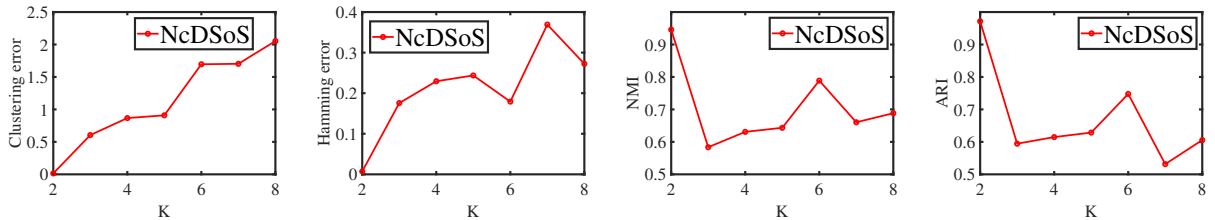


(e) Lazega law firm

(f) Lazega law firm

(g) Lazega law firm

(h) Lazega law firm



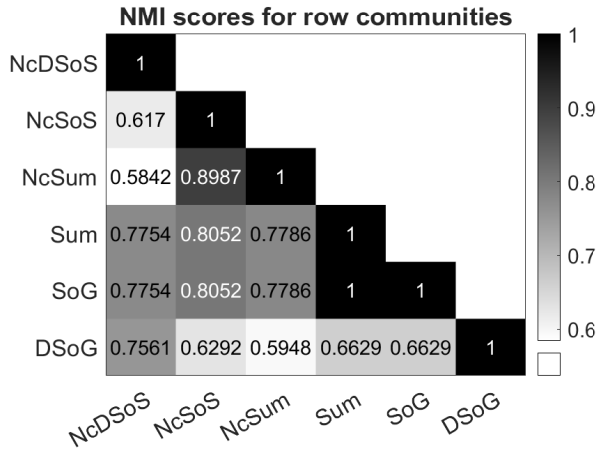
(i) C.elegans

(j) C.elegans

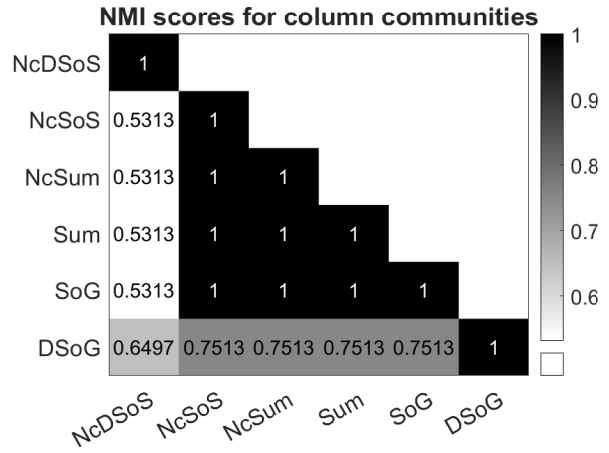
(k) C.elegans

(l) C.elegans

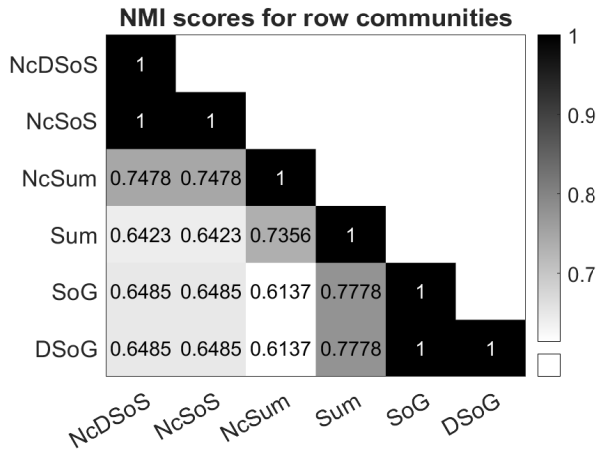
Figure 9: Four indices evaluating the difference between row clusters and column clusters against K for real data used in this paper, where row clusters and column clusters are obtained from our NcDSoS method.



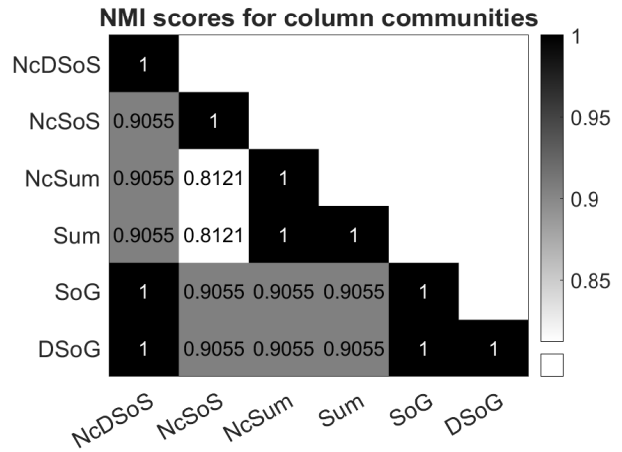
(a) Vickers Chan 7thGraders



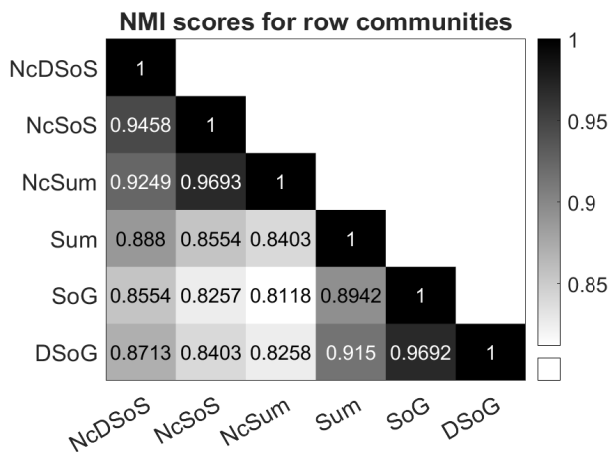
(b) Vickers Chan 7thGraders



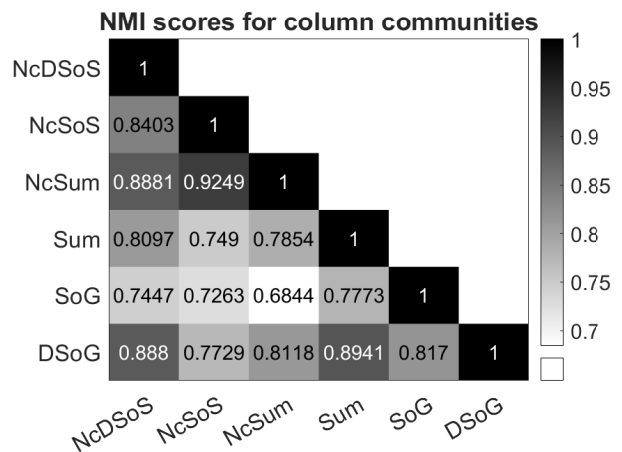
(c) Lazega law firm



(d) Lazega law firm



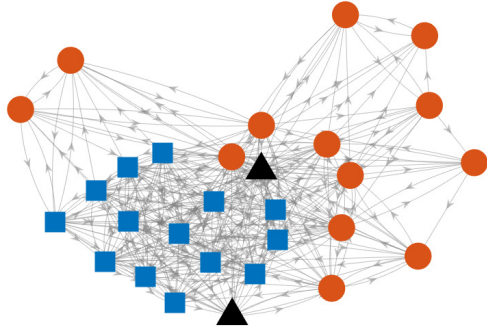
(e) C.elegans



(f) C.elegans

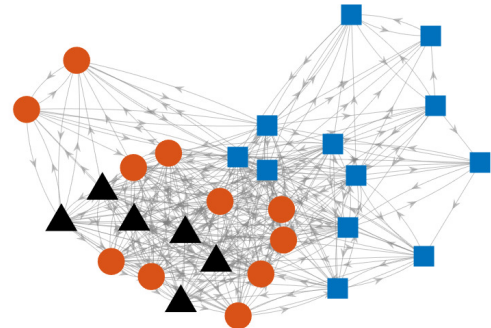
Figure 10: The pairwise comparison of NMI scores among 6 community detection approaches for both row and column communities of real-world multi-layer directed networks considered in this paper, where we set K as 3, 2, and 2 for Vickers Chan 7thGraders, Lazega law firm, and C.elegans, respectively.

Row communities of Layer 1



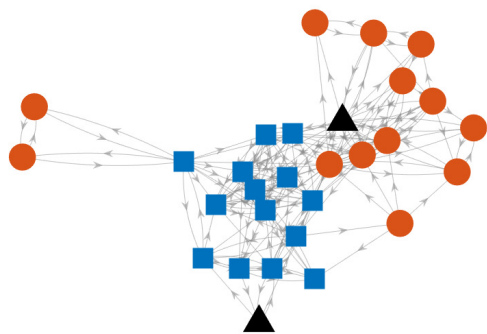
(a)

Column communities of Layer 1



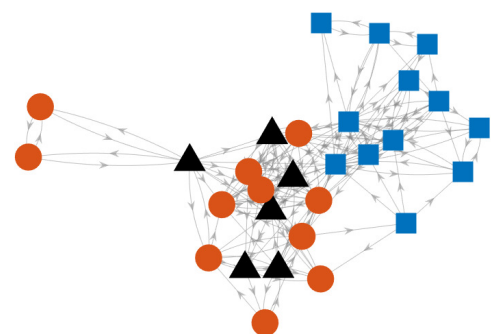
(b)

Row communities of Layer 2



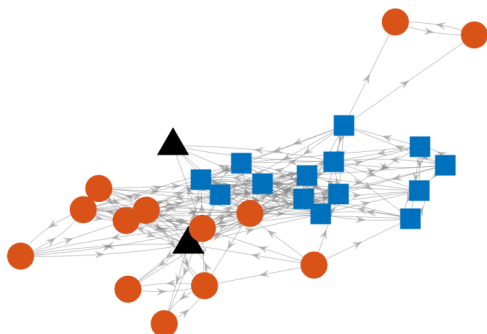
(c)

Column communities of Layer 2



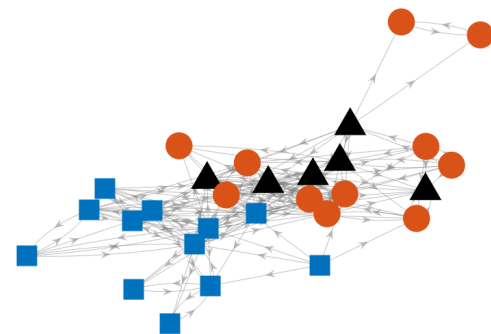
(d)

Row communities of Layer 3



(e)

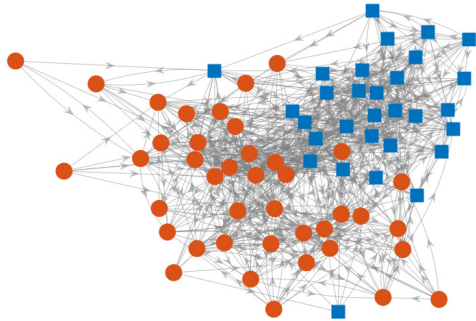
Column communities of Layer 3



(f)

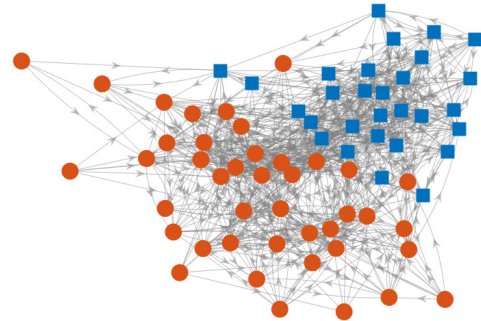
Figure 11: Visualization of communities detected by the NcDSoS algorithm when the number of communities K is 3 for Vickers Chan 7thGraders. Nodes that possess identical color and shape belong to the same estimated community.

Row communities of Layer 1



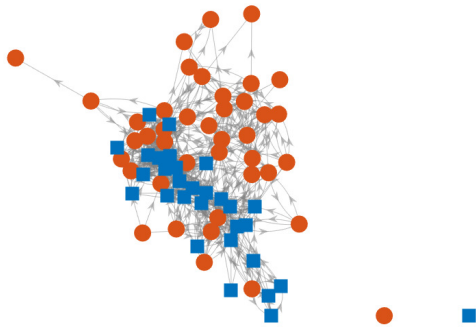
(a)

Column communities of Layer 1



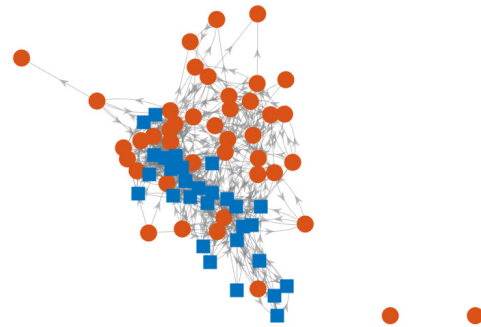
(b)

Row communities of Layer 2



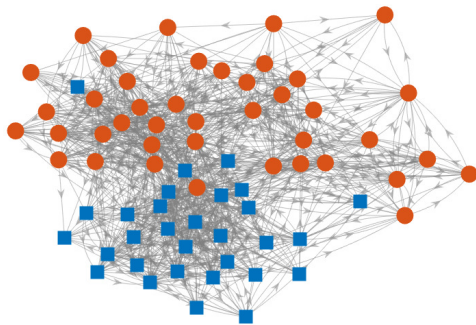
(c)

Column communities of Layer 2



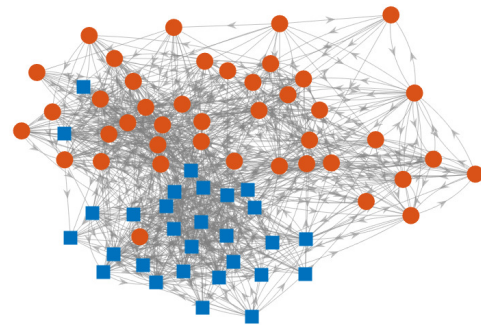
(d)

Row communities of Layer 3



(e)

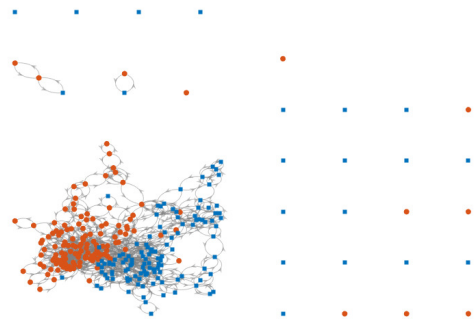
Column communities of Layer 3



(f)

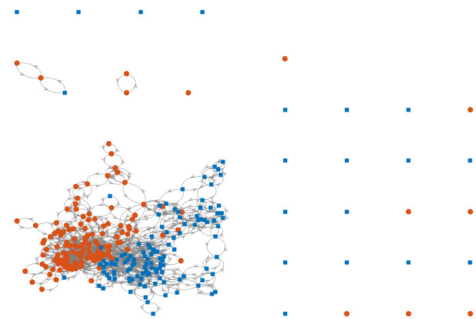
Figure 12: Visualization of communities detected by the NcDSoS algorithm when the number of communities K is 2 for Lazega law firm. Nodes that possess identical color and shape belong to the same estimated community.

Row communities of Layer 1



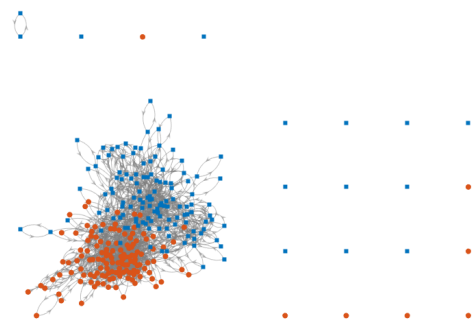
(a)

Column communities of Layer 1



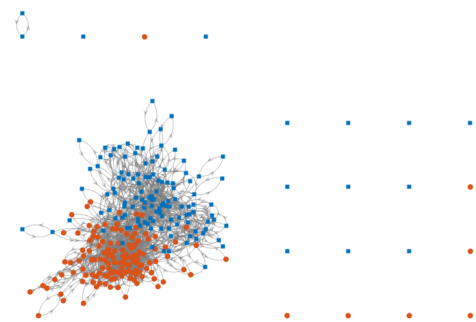
(b)

Row communities of Layer 2



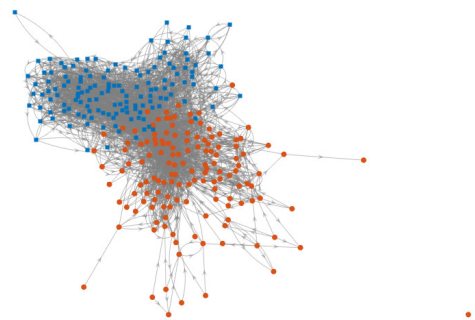
(c)

Column communities of Layer 2



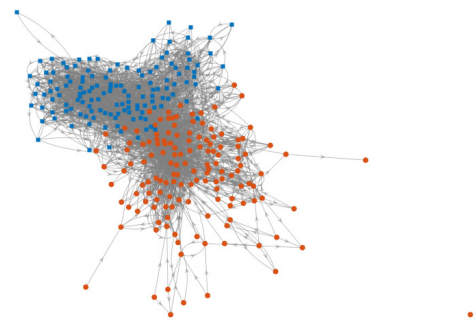
(d)

Row communities of Layer 3



(e)

Column communities of Layer 3



(f)

intersection of theory and practice, offering both a solid methodological foundation and practical insights into the analysis of complex network systems.

To further enhance the accuracy and applicability of the proposed model and algorithm, future research could explore the integration of additional network features, such as node attributes. This would allow for a more comprehensive representation of the network structure, potentially leading to improved performance (Binkiewicz et al., 2017; Chunaev, 2020; Cai et al., 2024). For instance, node attributes could capture information about the type or location of nodes, providing a richer understanding of their roles and interactions within the network. Additionally, extending the framework to other types of networks, such as weighted networks, represents a promising avenue for future research. Weighted networks incorporate edge weights that represent the strength or importance of connections, providing a richer representation of network interactions (Newman, 2004; Opsahl & Panzarasa, 2009; Qing & Wang, 2024). Adapting the model and algorithm to handle weighted networks would enable the analysis of a wider range of network systems, such as social networks with varying connection strengths. Finally, accelerating the algorithm to handle larger-scale networks is a crucial next step. Enhancing the scalability of the algorithm would allow for the analysis of even more complex network systems, providing valuable insights into their structure. This acceleration could involve subsampling techniques and approximation algorithms (Deng et al., 2024; Guo et al., 2023).

CRediT authorship contribution statement

Huan Qing: Conceptualization; Data curation; Formal analysis; Funding acquisition; Methodology; Project administration; Resources; Software; Validation; Visualization; Writing-original draft; Writing-review & editing.

Declaration of competing interest

The author declares no competing interests.

Data availability

Data and code will be made available on request.

Acknowledgements

H.Q. was sponsored by the Scientific Research Foundation of Chongqing University of Technology (Grant No: 0102240003) and the Natural Science Foundation of Chongqing, China (Grant No: CSTB2023NSCQ-LZX0048).

Appendix A. Proofs

Appendix A.1. Proof of Lemma 1

Proof. Recall that $\Omega_l = \Theta_r Z_r B_l Z_c' \Theta_c$ for each $l \in [L]$, we have $\tilde{S}_r = \sum_{l \in [L]} \Omega_l \Omega_l' = \sum_{l \in [L]} \Theta_r Z_r B_l Z_c' \Theta_c^2 Z_c B_l' Z_r' \Theta_r = \Theta_r Z_r (\sum_{l \in [L]} B_l Z_c' \Theta_c^2 Z_c B_l') Z_r' \Theta_r = U_r \Lambda_r U_r'$, which gives that $U_r = \Theta_r Z_r (\sum_{l \in [L]} B_l Z_c' \Theta_c^2 Z_c B_l') Z_r' \Theta_r U_r \Lambda_r^{-1}$. Set $X_r = (\sum_{l \in [L]} B_l Z_c' \Theta_c^2 Z_c B_l') Z_r' \Theta_r U_r \Lambda_r^{-1}$, we have $U_r = \Theta_r Z_r X_r$. Thus, $U_r^*(i_r, :) = \frac{U_r(i_r, :)}{\|U_r(i_r, :)\|_F} = \frac{\Theta_r(i_r, i_r) Z_r(i_r, :)}{\|\Theta_r(i_r, i_r) Z_r(i_r, :)\|_F} = \frac{Z_r(i_r, :)}{\|Z_r(i_r, :)\|_F}$, which suggests that $U_r^*(i_r, :) = U_r^*(\tilde{i}_r, :)$ if and only if $Z_r(i_r, :) = Z_r(\tilde{i}_r, :)$ for $i_r \in [n_r], \tilde{i}_r \in [n_r]$. Because $(\Theta_c Z_c)'(\Theta_c Z_c)$ is a positive definite diagonal matrix, $\text{rank}(\sum_{l \in [L]} B_l (\Theta_c Z_c)'(\Theta_c Z_c) B_l') = \text{rank}(\sum_{l \in [L]} B_l B_l')$. Therefore, when $\sum_{l \in [L]} B_l B_l'$ is full rank (i.e., $K = K_r$), Lemma 3 in (Qing & Wang, 2023) gives that $\|U_r^*(i_r, :) - U_r^*(\tilde{i}_r, :)\| = \sqrt{2}$ if $Z_r(i_r, :) \neq Z_r(\tilde{i}_r, :)$. The rest proof for U_c^* is similar to that of U_r^* , and we omit it here. \square

Appendix A.2. Proof of Lemma 2

Proof. Firstly, we bound $\|S_r - \tilde{S}_r\|$. Let $E_r^{(ij)}$ be an $n_r \times n_r$ matrix such that its (i, j) -th element is 1 while all the other entries are zeros for $i \in [n_r], j \in [n_r]$. We decompose $S_r - \tilde{S}_r$ into two parts:

$$\begin{aligned}
S_r - \tilde{S}_r &= \sum_{l \in [L]} (A_l A_l' - D_l^r - \Omega_l \Omega_l') = \sum_{l \in [L]} \sum_{i \in [n_r]} \sum_{j \in [n_r]} \sum_{m \in [n_c]} (A_l(i, m) A_l(j, m) - \Omega_l(i, m) \Omega_l(j, m)) E_r^{(ij)} - \sum_{l \in [L]} D_l^r \\
&= \sum_{l \in [L]} \sum_{i \in [n_r], j \in [n_r], i \neq j} \sum_{m \in [n_c]} (A_l(i, m) A_l(j, m) - \Omega_l(i, m) \Omega_l(j, m)) E_r^{(ij)} + \sum_{l \in [L]} \sum_{m \in [n_c]} \sum_{i \in [n_r]} (A_l^2(i, m) - \Omega_l^2(i, m)) E_r^{(ii)} - \sum_{l \in [L]} D_l^r \\
&= \sum_{l \in [L]} \sum_{i \in [n_r], j \in [n_r], i \neq j} \sum_{m \in [n_c]} (A_l(i, m) A_l(j, m) - \Omega_l(i, m) \Omega_l(j, m)) E_r^{(ij)} + \sum_{l \in [L]} \sum_{m \in [n_c]} \sum_{i \in [n_r]} (A_l(i, m) - \Omega_l^2(i, m)) E_r^{(ii)} - \sum_{l \in [L]} D_l^r \\
&= \sum_{l \in [L]} \sum_{i \in [n_r], j \in [n_r], i \neq j} \sum_{m \in [n_c]} (A_l(i, m) A_l(j, m) - \Omega_l(i, m) \Omega_l(j, m)) E_r^{(ij)} - \sum_{l \in [L]} \sum_{m \in [n_c]} \sum_{i \in [n_r]} \Omega_l^2(i, m) E_r^{(ii)} + \sum_{l \in [L]} \sum_{i \in [n_r]} \sum_{m \in [n_c]} A_l(i, m) E_r^{(ii)} - \sum_{l \in [L]} D_l^r \\
&= \sum_{l \in [L]} \sum_{i \in [n_r], j \in [n_r], i \neq j} \sum_{m \in [n_c]} (A_l(i, m) A_l(j, m) - \Omega_l(i, m) \Omega_l(j, m)) E_r^{(ij)} - \sum_{l \in [L]} \sum_{m \in [n_c]} \sum_{i \in [n_r]} \Omega_l^2(i, m) E_r^{(ii)} + \sum_{l \in [L]} D_l^r - \sum_{l \in [L]} D_l^r \\
&= \underbrace{\sum_{l \in [L]} \sum_{i \in [n_r], j \in [n_r], i \neq j} \sum_{m \in [n_c]} (A_l(i, m) A_l(j, m) - \Omega_l(i, m) \Omega_l(j, m)) E_r^{(ij)}}_{R1} - \underbrace{\sum_{l \in [L]} \sum_{m \in [n_c]} \sum_{i \in [n_r]} \Omega_l^2(i, m) E_r^{(ii)}}_{R2}.
\end{aligned}$$

$S_r - \tilde{S}_r = R1 - R2$ gives

$$\begin{aligned}
\|S_r - \tilde{S}_r\| &= \|R1 - R2\| \leq \|R1\| + \|R2\| = \|R1\| + \left\| \sum_{l \in [L]} \sum_{m \in [n_c]} \sum_{i \in [n_r]} \Omega_l^2(i, m) E_r^{(ii)} \right\| \\
&= \|R1\| + \max_{i \in [n_r]} \sum_{l \in [L]} \sum_{m \in [n_c]} \Omega_l^2(i, m) \\
&\leq \|R1\| + \max_{i \in [n_r]} \sum_{l \in [L]} \sum_{m \in [n_c]} \theta_r^2(i) \theta_c^2(m) \leq \|R1\| + \theta_{r, \max}^2 \sum_{l \in [L]} \sum_{m \in [n_c]} \theta_c^2(m) = \|R1\| + \theta_{r, \max}^2 \|\theta_c\|_F^2 L.
\end{aligned}$$

Next, we bound $\|R1\|$ by using Theorem 1.6 (the rectangular case of matrix Bernstein inequality) (Tropp, 2012). We write this theorem below.

Theorem 2. (Theorem 1.6 of (Tropp, 2012)) Consider a finite sequence $\{X_k\}$ of independent, random matrices with dimensions $d_1 \times d_2$. Suppose that each random matrix satisfies

$$\mathbb{E}[X_k] = 0 \text{ and } \|X_k\| \leq R \text{ almost surely.}$$

Define $\sigma^2 := \max\{\|\sum_k \mathbb{E}[X_k X_k']\|, \|\sum_k \mathbb{E}[X_k' X_k]\|\}$. Then, for all $t \geq 0$,

$$\mathbb{P}\left(\left\|\sum_k X_k\right\| \geq t\right) \leq (d_1 + d_2) \cdot \exp\left(\frac{-t^2/2}{\sigma^2 + Rt/3}\right).$$

Set $X_r^{(ijml)} = (A_l(i, m) A_l(j, m) - \Omega_l(i, m) \Omega_l(j, m)) E_r^{(ij)}$ for $i \in [n_r], j \in [n_r], i \neq j, m \in [n_c], l \in [L]$. We have $R1 = \sum_{l \in [L]} \sum_{i \in [n_r], j \in [n_r], i \neq j} \sum_{m \in [n_c]} X_r^{(ijml)}$. Note that although $R1$ is symmetric, $X_r^{(ijml)}$ is asymmetric and we need the rectangular case of matrix Bernstein to bound $\|R1\|$. The following results hold.

- $\mathbb{E}[X_r^{(ijml)}] = 0$ since $A_l(i, m)$ and $A_l(j, m)$ are independent when $i \neq j$.
 - $\|X_r^{(ijml)}\| = |A_l(i, m) A_l(j, m) - \Omega_l(i, m) \Omega_l(j, m)| \leq 1$. Set $R_r = 1$.
 - Set $\sigma_r^2 = \max\{\|\sum_{l \in [L]} \sum_{i \in [n_r], j \in [n_r], i \neq j} \sum_{m \in [n_c]} \mathbb{E}[X_r^{(ijml)} (X_r^{(ijml)})']\|, \|\sum_{l \in [L]} \sum_{i \in [n_r], j \in [n_r], i \neq j} \sum_{m \in [n_c]} \mathbb{E}[(X_r^{(ijml)})' X_r^{(ijml)}]\|\}$.
- Under the multi-layer DC-ScBM, for the term $\|\sum_{l \in [L]} \sum_{i \in [n_r], j \in [n_r], i \neq j} \sum_{m \in [n_c]} \mathbb{E}[X_r^{(ijml)} (X_r^{(ijml)})']\|$, we have

$$\left\| \sum_{l \in [L]} \sum_{i \in [n_r], j \in [n_r], i \neq j} \sum_{m \in [n_c]} \mathbb{E}[(A_l(i, m) A_l(j, m) - \Omega_l(i, m) \Omega_l(j, m))^2 E_r^{(ii)}] \right\|$$

$$\begin{aligned}
&= \left\| \sum_{l \in [L]} \sum_{i \in [n_r], j \in [n_r], i \neq j} \sum_{m \in [n_c]} E_r^{(ii)} \mathbb{E}[A_l^2(i, m)A_l^2(j, m) - 2A_l(i, m)A_l(j, m)\Omega_l(i, m)\Omega_l(j, m) + \Omega_l^2(i, m)\Omega_l^2(j, m)] \right\| \\
&= \left\| \sum_{l \in [L]} \sum_{i \in [n_r], j \in [n_r], i \neq j} \sum_{m \in [n_c]} E_r^{(ii)} (\mathbb{E}[A_l^2(i, m)A_l^2(j, m)] - \Omega_l^2(i, m)\Omega_l^2(j, m)) \right\| \\
&= \left\| \sum_{l \in [L]} \sum_{i \in [n_r], j \in [n_r], i \neq j} \sum_{m \in [n_c]} E_r^{(ii)} (\mathbb{E}[A_l(i, m)A_l(j, m)] - \Omega_l^2(i, m)\Omega_l^2(j, m)) \right\| \\
&= \left\| \sum_{l \in [L]} \sum_{i \in [n_r], j \in [n_r], i \neq j} \sum_{m \in [n_c]} E_r^{(ii)} (\mathbb{E}[A_l(i, m)]\mathbb{E}[A_l(j, m)] - \Omega_l^2(i, m)\Omega_l^2(j, m)) \right\| \\
&= \left\| \sum_{l \in [L]} \sum_{i \in [n_r], j \in [n_r], i \neq j} \sum_{m \in [n_c]} E_r^{(ii)} \Omega_l(i, m)\Omega_l(j, m)(1 - \Omega_l(i, m)\Omega_l(j, m)) \right\| \\
&= \max_{i \in [n_r]} \sum_{l \in [L]} \sum_{j \in [n_r], j \neq i} \sum_{m \in [n_c]} \Omega_l(i, m)\Omega_l(j, m)(1 - \Omega_l(i, m)\Omega_l(j, m)) \\
&\leq \max_{i \in [n_r]} \sum_{l \in [L]} \sum_{j \in [n_r], j \neq i} \sum_{m \in [n_c]} \Omega_l(i, m)\Omega_l(j, m) \\
&\leq \max_{i \in [n_r]} \sum_{l \in [L]} \sum_{j \in [n_r], j \neq i} \sum_{m \in [n_c]} \theta_r(i)\theta_c^2(m)\theta_r(j) \leq \theta_{r, \max} \sum_{l \in [L]} \sum_{j \in [n_r]} \sum_{m \in [n_c]} \theta_c^2(m)\theta_r(j) = \theta_{r, \max} \|\theta_r\|_1 \|\theta_c\|_F^2 L.
\end{aligned}$$

Similarly, we have $\left\| \sum_{l \in [L]} \sum_{i \in [n_r], j \in [n_r], i \neq j} \sum_{m \in [n_c]} \mathbb{E}[(X_r^{(ijml)})' X_r^{(ijml)}] \right\| \leq \theta_{r, \max} \|\theta_r\|_1 \|\theta_c\|_F^2 L$. Hence, $\sigma_r^2 \leq \theta_{r, \max} \|\theta_r\|_1 \|\theta_c\|_F^2 L$. For any $t_r \geq 0$, Theorem 2 gives

$$\mathbb{P}(\|R1\| \geq t_r) \leq 2n_r \cdot \exp\left(\frac{-t_r^2/2}{\sigma_r^2 + R_r t_r/3}\right) \leq 2n_r \cdot \exp\left(\frac{-t_r^2/2}{\theta_{r, \max} \|\theta_r\|_1 \|\theta_c\|_F^2 L + t_r/3}\right).$$

Set $t_r = \frac{\alpha+1+\sqrt{(\alpha+1)(\alpha+19)}}{3} \sqrt{\theta_{r, \max} \|\theta_r\|_1 \|\theta_c\|_F^2 L \log(n_r + n_c + L)}$ for any $\alpha \geq 0$. By Assumption 1, we get

$$\mathbb{P}(\|R1\| \geq t_r) \leq 2n_r \cdot \exp(-(\alpha+1)\log(n_r + n_c + L)) \frac{1}{\left(\frac{18}{(\sqrt{\alpha+1} + \sqrt{\alpha+19})^2} + \frac{2\sqrt{\alpha+1}}{\sqrt{\alpha+1} + \sqrt{\alpha+19}} \sqrt{\frac{\log(n_r + n_c + L)}{\theta_{r, \max} \|\theta_r\|_1 \|\theta_c\|_F^2 L}}\right)} \leq \frac{2n_r}{(n_r + n_c + L)^{\alpha+1}} < \frac{2}{(n_r + n_c + L)^\alpha}.$$

Setting $\alpha = 1$, with probability at least $1 - o\left(\frac{1}{n_r + n_c + L}\right)$, we have

$$\|S_r - \tilde{S}_r\| = O\left(\sqrt{\theta_{r, \max} \|\theta_r\|_1 \|\theta_c\|_F^2 L \log(n_r + n_c + L)}\right) + O(\theta_{r, \max}^2 \|\theta_c\|_F^2 L).$$

Secondly, we bound $\|S_c - \tilde{S}_c\|$. Let $E_c^{(ij)}$ be an $n_c \times n_c$ matrix with its (i, j) -th entry being 1 and all the other entries being zeros for $i \in [n_c], j \in [n_c]$. We have

$$\begin{aligned}
S_c - \tilde{S}_c &= \sum_{l \in [L]} (A_l' A_l - D_l^c - \Omega_l' \Omega_l) = \sum_{l \in [L]} \sum_{i \in [n_c]} \sum_{j \in [n_c]} \sum_{m \in [n_r]} (A_l(m, i)A_l(m, j) - \Omega_l(m, i)\Omega_l(m, j)) E_c^{(ij)} - \sum_{l \in [L]} D_l^c \\
&= \underbrace{\sum_{l \in [L]} \sum_{i \in [n_c], j \in [n_c], i \neq j} \sum_{m \in [n_r]} (A_l(m, i)A_l(m, j) - \Omega_l(m, i)\Omega_l(m, j)) E_c^{(ij)}}_{C1} - \underbrace{\sum_{l \in [L]} \sum_{m \in [n_r]} \sum_{i \in [n_c]} \Omega_l^2(m, i) E_c^{(ii)}}_{C2},
\end{aligned}$$

which gives

$$\begin{aligned}
\|S_c - \tilde{S}_c\| &= \|C1 - C2\| \leq \|C1\| + \|C2\| = \|C1\| + \left\| \sum_{l \in [L]} \sum_{m \in [n_r]} \sum_{i \in [n_c]} \Omega_l^2(m, i) E_c^{(ii)} \right\| \\
&= \|C1\| + \max_{i \in [n_c]} \sum_{l \in [L]} \sum_{m \in [n_r]} \Omega_l^2(m, i) \\
&\leq \|C1\| + \max_{i \in [n_c]} \sum_{l \in [L]} \sum_{m \in [n_r]} \theta_c^2(i)\theta_r^2(m) \leq \|C1\| + \theta_{c, \max}^2 \sum_{l \in [L]} \sum_{m \in [n_r]} \theta_r^2(m) = \|C1\| + \theta_{c, \max}^2 \|\theta_r\|_F^2 L.
\end{aligned}$$

As long as we obtain an upper bound of $\|C1\|$, we can bound $\|S_c - \tilde{S}_c\|$.

Setting $X_c^{(ijml)} = (A_l(m, i)A_l(m, j) - \Omega_l(m, i)\Omega_l(m, j))E_c^{(ij)}$ (for $i \in [n_c], j \in [n_c], i \neq j, m \in [n_r], l \in [L]$) gives $C1 = \sum_{l \in [L]} \sum_{i \in [n_c], j \in [n_c], i \neq j} \sum_{m \in [n_r]} X_c^{(ijml)}$. We have the following conclusions:

- $\mathbb{E}[X_c^{(ijml)}] = 0$ because $A_l(m, i)$ and $A_l(m, j)$ are independent when $i \neq j$.
- $\|X_c^{(ijml)}\| \leq 1$. Set $R_c = 1$.
- Set $\sigma_c^2 = \max\{\|\sum_{l \in [L]} \sum_{i \in [n_c], j \in [n_c], i \neq j} \sum_{m \in [n_r]} \mathbb{E}[X_c^{(ijml)}(X_c^{(ijml)})']\|, \|\sum_{l \in [L]} \sum_{i \in [n_c], j \in [n_c], i \neq j} \sum_{m \in [n_r]} \mathbb{E}[(X_c^{(ijml)})'(X_c^{(ijml)})]\|\}$. For $\|\sum_{l \in [L]} \sum_{i \in [n_c], j \in [n_c], i \neq j} \sum_{m \in [n_r]} \mathbb{E}[X_c^{(ijml)}(X_c^{(ijml)})']\|$, we have

$$\begin{aligned}
& \left\| \sum_{l \in [L]} \sum_{i \in [n_c], j \in [n_c], i \neq j} \sum_{m \in [n_r]} \mathbb{E}[(A_l(m, i)A_l(m, j) - \Omega_l(m, i)\Omega_l(m, j))^2 E_c^{(ii)}] \right\| \\
&= \left\| \sum_{l \in [L]} \sum_{i \in [n_c], j \in [n_c], i \neq j} \sum_{m \in [n_r]} E_c^{(ii)} \Omega_l(m, i)\Omega_l(m, j)(1 - \Omega_l(m, i)\Omega_l(m, j)) \right\| \\
&= \max_{i \in [n_c]} \sum_{l \in [L]} \sum_{j \in [n_c], j \neq i} \sum_{m \in [n_r]} \Omega_l(m, i)\Omega_l(m, j)(1 - \Omega_l(m, i)\Omega_l(m, j)) \\
&\leq \max_{i \in [n_c]} \sum_{l \in [L]} \sum_{j \in [n_c], j \neq i} \sum_{m \in [n_r]} \Omega_l(m, i)\Omega_l(m, j) \\
&\leq \max_{i \in [n_c]} \sum_{l \in [L]} \sum_{j \in [n_c], j \neq i} \sum_{m \in [n_r]} \theta_c(i)\theta_r^2(m)\theta_c(j) \leq \theta_{c, \max} \sum_{l \in [L]} \sum_{j \in [n_c]} \sum_{m \in [n_r]} \theta_r^2(m)\theta_c(j) = \theta_{c, \max} \|\theta_c\|_1 \|\theta_r\|_F^2 L.
\end{aligned}$$

Following a similar analysis, we get $\|\sum_{l \in [L]} \sum_{i \in [n_c], j \in [n_c], i \neq j} \sum_{m \in [n_r]} \mathbb{E}[(X_c^{(ijml)})'(X_c^{(ijml)})]\| \leq \theta_{c, \max} \|\theta_c\|_1 \|\theta_r\|_F^2 L$. Thus, $\sigma_c^2 \leq \theta_{c, \max} \|\theta_c\|_1 \|\theta_r\|_F^2 L$. For any $t_c \geq 0$, by Theorem 2, we have

$$\mathbb{P}(\|C1\| \geq t_c) \leq 2n_c \cdot \exp\left(\frac{-t_c^2/2}{\sigma_c^2 + R_c t_c/3}\right) \leq 2n_c \cdot \exp\left(\frac{-t_c^2/2}{\theta_{c, \max} \|\theta_c\|_1 \|\theta_r\|_F^2 L + t_c/3}\right).$$

Set $t_c = \frac{\alpha+1+\sqrt{(\alpha+1)(\alpha+19)}}{3} \sqrt{\theta_{c, \max} \|\theta_c\|_1 \|\theta_r\|_F^2 L \log(n_r + n_c + L)}$ for any $\alpha \geq 0$. By Assumption 1, we obtain

$$\mathbb{P}(\|C1\| \geq t_c) \leq 2n_c \cdot \exp(-(\alpha+1)\log(n_r + n_c + L)) \frac{1}{\frac{18}{(\alpha+1+\sqrt{(\alpha+1)(\alpha+19)})^2} + \frac{2\sqrt{\alpha+1}}{\sqrt{\alpha+1+\sqrt{\alpha+19}}} \sqrt{\frac{\log(n_r+n_c+L)}{\theta_{c, \max} \|\theta_c\|_1 \|\theta_r\|_F^2 L}}} \leq \frac{2n_c}{(n_r + n_c + L)^{\alpha+1}} < \frac{2}{(n_r + n_c + L)^\alpha}.$$

Letting $\alpha = 1$, with probability at least $1 - o(\frac{1}{n_r+n_c+L})$, we have

$$\|S_c - \tilde{S}_c\| = O\left(\sqrt{\theta_{c, \max} \|\theta_c\|_1 \|\theta_r\|_F^2 L \log(n_r + n_c + L)}\right) + O(\theta_{c, \max}^2 \|\theta_r\|_F^2 L).$$

□

Appendix A.3. Proof of Theorem 1

Proof. By Lemma 5.1 (Lei & Rinaldo, 2015), there are two orthogonal matrices $Q_r \in \mathbb{R}^{K_r \times K_r}$ and $Q_c \in \mathbb{R}^{K_c \times K_c}$ such that

$$\|\hat{U}_r Q_r - U_r\|_F \leq \frac{2\sqrt{2K_r} \|S_r - \tilde{S}_r\|}{|\lambda_{K_r}(\tilde{S}_r)|} \text{ and } \|\hat{U}_c Q_c - U_c\|_F \leq \frac{2\sqrt{2K_c} \|S_c - \tilde{S}_c\|}{|\lambda_{K_c}(\tilde{S}_c)|}.$$

Combine Assumption 2 with the truth that $Z_c' \Theta_c^2 Z_c$ is a diagonal matrix, we get

$$|\lambda_{K_r}(\tilde{S}_r)| = |\lambda_{K_r}\left(\sum_{l \in [L]} \Theta_r Z_r B_l Z_c' \Theta_c^2 Z_c B_l' Z_r' \Theta_r\right)| = |\lambda_{K_r}(\Theta_r Z_r \left(\sum_{l \in [L]} B_l Z_c' \Theta_c^2 Z_c B_l'\right) Z_r' \Theta_r)| \geq \lambda_{K_r}^2(\Theta_r) \lambda_{K_r}(Z_r' Z_r) |\lambda_{K_r}\left(\sum_{l \in [L]} B_l Z_c' \Theta_c^2 Z_c B_l'\right)|$$

$$\begin{aligned}
&= O(\lambda_{K_r}^2(\Theta_r)\lambda_{K_r}^2(\Theta_c)\lambda_{K_r}(Z_r'Z_r)\lambda_{K_r}(Z_c'Z_c)|\lambda_{K_r}(\sum_{l \in [L]} B_l B_l')|) = \lambda_{K_r}^2(\Theta_r)\lambda_{K_r}^2(\Theta_c)\lambda_{K_r}(Z_r'Z_r)\lambda_{K_r}(Z_c'Z_c)O(|\lambda_{K_r}(\sum_{l \in [L]} B_l B_l')|) \\
&\geq \theta_{r,\min}^2 \theta_{c,\min}^2 n_{r,\min} n_{c,\min} O(\lambda_{K_r}(\sum_{l \in [L]} B_l B_l')) = O(\theta_{r,\min}^2 \theta_{c,\min}^2 n_{r,\min} n_{c,\min} L).
\end{aligned}$$

Similarly, we have $|\lambda_{K_c}(\tilde{S}_c)| \geq O(\theta_{r,\min}^2 \theta_{c,\min}^2 n_{r,\min} n_{c,\min} L)$. Thus, $\|\hat{U}_r Q_r - U_r\|_F = O(\frac{\sqrt{K_r} \|S_r - \tilde{S}_r\|}{\theta_{r,\min}^2 \theta_{c,\min}^2 n_{r,\min} n_{c,\min} L})$ and $\|\hat{U}_c Q_c - U_c\|_F = O(\frac{\sqrt{K_c} \|S_c - \tilde{S}_c\|}{\theta_{r,\min}^2 \theta_{c,\min}^2 n_{r,\min} n_{c,\min} L})$. Set $\mu_r = \min_{i \in [n_r]} \|U_r(i, :)\|_F$ and $\mu_c = \min_{j \in [n_c]} \|U_c(j, :)\|_F$. By basic algebra, we have $\|\hat{U}_r^* Q_r - U_r^*\|_F \leq \frac{2\|\hat{U}_r Q_r - U_r\|_F}{\mu_r}$ and $\|\hat{U}_c^* Q_c - U_c^*\|_F \leq \frac{2\|\hat{U}_c Q_c - U_c\|_F}{\mu_c}$. According to the proof of Lemma 7 (Qing & Wang, 2023), we have $\frac{1}{\mu_r} \leq \frac{\theta_{r,\max} \sqrt{n_{r,\max}}}{\theta_{r,\min}}$ and $\frac{1}{\mu_c} \leq \frac{\theta_{c,\max} \sqrt{n_{c,\max}}}{\theta_{c,\min}}$. Then, we get

$$\|\hat{U}_r^* Q_r - U_r^*\|_F = O\left(\frac{\theta_{r,\max} \sqrt{K_r n_{r,\max}} \|S_r - \tilde{S}_r\|}{\theta_{r,\min}^3 \theta_{c,\min}^2 n_{r,\min} n_{c,\min} L}\right) \text{ and } \|\hat{U}_c^* Q_c - U_c^*\|_F = O\left(\frac{\theta_{c,\max} \sqrt{K_c n_{c,\max}} \|S_c - \tilde{S}_c\|}{\theta_{r,\min}^2 \theta_{c,\min}^3 n_{r,\min} n_{c,\min} L}\right).$$

By Lemma 1 and the proof of Theorem 2 (Qing & Wang, 2023), we have

$$\begin{aligned}
\hat{f}_r &= O\left(\frac{K_r}{n_{r,\min}} \|\hat{U}_r^* Q_r - U_r^*\|_F^2\right) = O\left(\frac{\theta_{r,\max}^2 K_r^2 n_{r,\max} \|S_r - \tilde{S}_r\|^2}{\theta_{r,\min}^6 \theta_{c,\min}^4 n_{r,\min}^3 n_{c,\min}^2 L^2}\right) \\
\hat{f}_c &= O\left(\frac{K_c}{n_{c,\min}} \|\hat{U}_c^* Q_c - U_c^*\|_F^2\right) = O\left(\frac{\theta_{c,\max}^2 K_c^2 n_{c,\max} \|S_c - \tilde{S}_c\|^2}{\theta_{r,\min}^4 \theta_{c,\min}^6 n_{r,\min}^2 n_{c,\min}^3 L^2}\right).
\end{aligned}$$

Based on Lemma 2, we have

$$\begin{aligned}
\hat{f}_r &= O\left(\frac{\theta_{r,\max}^3 K_r^2 n_{r,\max} \|\theta_r\|_1 \|\theta_c\|_1^2 \log(n_r + n_c + L)}{\theta_{r,\min}^6 \theta_{c,\min}^4 n_{r,\min}^3 n_{c,\min}^2 L}\right) + O\left(\frac{\theta_{r,\max}^6 K_r^2 n_{r,\max} \|\theta_c\|_1^4}{\theta_{r,\min}^6 \theta_{c,\min}^4 n_{r,\min}^3 n_{c,\min}^2}\right) \\
\hat{f}_c &= O\left(\frac{\theta_{c,\max}^3 K_c^2 n_{c,\max} \|\theta_c\|_1 \|\theta_r\|_1^2 \log(n_r + n_c + L)}{\theta_{r,\min}^4 \theta_{c,\min}^6 n_{r,\min}^2 n_{c,\min}^3 L}\right) + O\left(\frac{\theta_{c,\max}^6 K_c^2 n_{c,\max} \|\theta_r\|_1^4}{\theta_{r,\min}^4 \theta_{c,\min}^6 n_{r,\min}^2 n_{c,\min}^3}\right).
\end{aligned}$$

□

References

- Bagrow, J. P. (2008). Evaluating local community methods in networks. *Journal of Statistical Mechanics: Theory and Experiment*, 2008, P05001.
- Bakken, T. E., Miller, J. A., Ding, S.-L., Sunkin, S. M., Smith, K. A., Ng, L., Szafer, A., Dalley, R. A., Royall, J. J., Lemon, T. et al. (2016). A comprehensive transcriptional map of primate brain development. *Nature*, 535, 367–375.
- Binkiewicz, N., Vogelstein, J. T., & Rohe, K. (2017). Covariate-assisted spectral clustering. *Biometrika*, 104, 361–377.
- Boccaletti, S., Bianconi, G., Criado, R., Del Genio, C. I., Gómez-Gardenes, J., Romance, M., Sendina-Nadal, I., Wang, Z., & Zanin, M. (2014). The structure and dynamics of multilayer networks. *Physics Reports*, 544, 1–122.
- Cai, J., Hao, J., Yang, H., Yang, Y., Zhao, X., Xun, Y., & Zhang, D. (2024). A new community detection method for simplified networks by combining structure and attribute information. *Expert Systems with Applications*, 246, 123103.
- Chen, B. L., Hall, D. H., & Chklovskii, D. B. (2006). Wiring optimization can relate neuronal structure and function. *Proceedings of the National Academy of Sciences*, 103, 4723–4728.
- Chen, Y., & Mo, D. (2022). Community detection for multilayer weighted networks. *Information Sciences*, 595, 119–141.
- Chunaev, P. (2020). Community detection in node-attributed social networks: a survey. *Computer Science Review*, 37, 100286.
- Danon, L., Diaz-Guilera, A., Duch, J., & Arenas, A. (2005). Comparing community structure identification. *Journal of Statistical Mechanics: Theory and Experiment*, 2005, P09008.
- De Domenico, M., Granell, C., Porter, M. A., & Arenas, A. (2016). The physics of spreading processes in multilayer networks. *Nature Physics*, 12, 901–906.
- De Domenico, M., Nicosia, V., Arenas, A., & Latora, V. (2015a). Structural reducibility of multilayer networks. *Nature Communications*, 6, 6864.
- De Domenico, M., Porter, M. A., & Arenas, A. (2015b). Muxviz: a tool for multilayer analysis and visualization of networks. *Journal of Complex Networks*, 3, 159–176.
- De Domenico, M., Solé-Ribalta, A., Cozzo, E., Kivela, M., Moreno, Y., Porter, M. A., Gómez, S., & Arenas, A. (2013). Mathematical formulation of multilayer networks. *Physical Review X*, 3, 041022.
- Deng, J., Huang, D., Ding, Y., Zhu, Y., Jing, B., & Zhang, B. (2024). Subsampling spectral clustering for stochastic block models in large-scale networks. *Computational Statistics & Data Analysis*, 189, 107835.

- Fan, X., Pensky, M., Yu, F., & Zhang, T. (2022). Alma: Alternating minimization algorithm for clustering mixture multilayer network. *Journal of Machine Learning Research*, 23, 1–46.
- Fortunato, S. (2010). Community detection in graphs. *Physics Reports*, 486, 75–174.
- Fortunato, S., & Hric, D. (2016). Community detection in networks: A user guide. *Physics Reports*, 659, 1–44.
- Girvan, M., & Newman, M. E. (2002). Community structure in social and biological networks. *Proceedings of the National Academy of Sciences*, 99, 7821–7826.
- Guo, X., Qiu, Y., Zhang, H., & Chang, X. (2023). Randomized spectral co-clustering for large-scale directed networks. *Journal of Machine Learning Research*, 24, 1–68.
- Han, Q., Xu, K., & Airoldi, E. (2015). Consistent estimation of dynamic and multi-layer block models. In *International Conference on Machine Learning* (pp. 1511–1520). PMLR.
- Holland, P. W., Laskey, K. B., & Leinhardt, S. (1983). Stochastic blockmodels: First steps. *Social Networks*, 5, 109–137.
- Huang, X., Chen, D., Ren, T., & Wang, D. (2021). A survey of community detection methods in multilayer networks. *Data Mining and Knowledge Discovery*, 35, 1–45.
- Hubert, L., & Arabie, P. (1985). Comparing partitions. *Journal of Classification*, 2, 193–218.
- Javed, M. A., Younis, M. S., Latif, S., Qadir, J., & Baig, A. (2018). Community detection in networks: A multidisciplinary review. *Journal of Network and Computer Applications*, 108, 87–111.
- Jin, J. (2015). Fast community detection by SCORE. *Annals of Statistics*, 43, 57–89.
- Jing, B.-Y., Li, T., Lyu, Z., & Xia, D. (2021). Community detection on mixture multilayer networks via regularized tensor decomposition. *Annals of Statistics*, 49, 3181–3205.
- Joseph, A., & Yu, B. (2016). Impact of regularization on spectral clustering. *Annals of Statistics*, 44, 1765–1791.
- Karrer, B., & Newman, M. E. (2011). Stochastic blockmodels and community structure in networks. *Physical Review E*, 83, 016107.
- Kim, J., & Lee, J.-G. (2015). Community detection in multi-layer graphs: A survey. *ACM SIGMOD Record*, 44, 37–48.
- Kiveliä, M., Arenas, A., Barthelemy, M., Gleeson, J. P., Moreno, Y., & Porter, M. A. (2014). Multilayer networks. *Journal of Complex Networks*, 2, 203–271.
- Latapy, M., Magnien, C., & Del Vecchio, N. (2008). Basic notions for the analysis of large two-mode networks. *Social Networks*, 30, 31–48.
- Lazega, E. (2001). *The collegial phenomenon: The social mechanisms of cooperation among peers in a corporate law partnership*. Oxford University Press, USA.
- Lei, J., Chen, K., & Lynch, B. (2020). Consistent community detection in multi-layer network data. *Biometrika*, 107, 61–73.
- Lei, J., & Lin, K. Z. (2023). Bias-adjusted spectral clustering in multi-layer stochastic block models. *Journal of the American Statistical Association*, 118, 2433–2445.
- Lei, J., & Rinaldo, A. (2015). Consistency of spectral clustering in stochastic block models. *Annals of Statistics*, 43, 215–237.
- Narayanan, M., Vetta, A., Schadt, E. E., & Zhu, J. (2010). Simultaneous clustering of multiple gene expression and physical interaction datasets. *PLoS Computational Biology*, 6, e1000742.
- Newman, M. E. (2004). Analysis of weighted networks. *Physical review E*, 70, 056131.
- Newman, M. E., & Girvan, M. (2004). Finding and evaluating community structure in networks. *Physical Review E*, 69, 026113.
- Opsahl, T., & Panzarasa, P. (2009). Clustering in weighted networks. *Social networks*, 31, 155–163.
- Papadopoulos, S., Kompatsiaris, Y., Vakali, A., & Spyridonos, P. (2012). Community detection in social media: Performance and application considerations. *Data Mining and Knowledge Discovery*, 24, 515–554.
- Papalexakis, E. E., Akoglu, L., & Ience, D. (2013). Do more views of a graph help? community detection and clustering in multi-graphs. In *Proceedings of the 16th International Conference on Information Fusion* (pp. 899–905). IEEE.
- Paul, S., & Chen, Y. (2016). Consistent community detection in multi-relational data through restricted multi-layer stochastic blockmodel. *Electronic Journal of Statistics*, 10, 3807 – 3870.
- Paul, S., & Chen, Y. (2020). Spectral and matrix factorization methods for consistent community detection in multi-layer networks. *Annals of Statistics*, 48, 230 – 250.
- Pilosof, S., Porter, M. A., Pascual, M., & Kéfi, S. (2017). The multilayer nature of ecological networks. *Nature Ecology & Evolution*, 1, 0101.
- Qing, H., & Wang, J. (2023). Community detection for weighted bipartite networks. *Knowledge-Based Systems*, 274, 110643.
- Qing, H., & Wang, J. (2024). Bipartite mixed membership distribution-free model. a novel model for community detection in overlapping bipartite weighted networks. *Expert Systems with Applications*, 235, 121088.
- Rohe, K., Qin, T., & Yu, B. (2016). Co-clustering directed graphs to discover asymmetries and directional communities. *Proceedings of the National Academy of Sciences*, 113, 12679–12684.
- Snijders, T. A., Pattison, P. E., Robins, G. L., & Handcock, M. S. (2006). New specifications for exponential random graph models. *Sociological Methodology*, 36, 99–153.
- Strehl, A., & Ghosh, J. (2002). Cluster ensembles—a knowledge reuse framework for combining multiple partitions. *Journal of Machine Learning Research*, 3, 583–617.
- Su, W., Guo, X., Chang, X., & Yang, Y. (2023). Spectral co-clustering in rank-deficient multi-layer stochastic co-block models. *arXiv preprint arXiv:2307.10572*, .
- Tropp, J. A. (2012). User-friendly tail bounds for sums of random matrices. *Foundations of Computational Mathematics*, 12, 389–434.
- Vasques Filho, D., & O’Neale, D. R. (2018). Degree distributions of bipartite networks and their projections. *Physical Review E*, 98, 022307.
- Vickers, M., & Chan, S. (1981). Representing classroom social structure. *Victoria Institute of Secondary Education, Melbourne*, .
- Vinh, N. X., Epps, J., & Bailey, J. (2009). Information theoretic measures for clusterings comparison: is a correction for chance necessary? In *Proceedings of the 26th annual International Conference on Machine Learning* (pp. 1073–1080).
- Zhang, J., & Cao, J. (2017). Finding common modules in a time-varying network with application to the drosophila melanogaster gene regulation network. *Journal of the American Statistical Association*, 112, 994–1008.